Fall 12-4-2015

Development of Semi-Circular Bending (SCB) Fracture Test for Bituminous Mixtures

Gabriel Nsengiyumva
University of Nebraska-Lincoln, gabriron01@huskers.unl.edu

DEVELOPMENT OF SEMI-CIRCULAR BENDING (SCB) FRACTURE TEST FOR BITUMINOUS MIXTURES.

by

Gabriel Nsengiyumva

A THESIS

Presented to the Faculty of

The Graduate College at the University of Nebraska

In Partial Fulfillment of Requirements

For the Degree of Master of Science

Major: Civil Engineering

Under the Supervision of Professor Yong-Rak Kim

Lincoln, Nebraska,

December, 2015

DEVELOPMENT OF SEMI-CIRCULAR BENDING (SCB) FRACTURE TEST FOR BITUMINOUS MIXTURES.

Gabriel Nsengiyumva, M.S.

University of Nebraska, 2015

Adviser: Yong-Rak Kim

Granted that most distresses in asphalt (flexible) concrete (AC) pavements are directly related to fracture, it becomes clear that identifying and characterizing fracture properties of AC mixtures is a critical step towards a better pavement design. This thesis examines the testing variables of a reliable and practical semicircular bending (SCB) test for evaluating the fracture characteristics of asphalt concrete mixtures at intermediate service temperature conditions. The first part of this thesis investigates the repeatability of the SCB fracture test method by integrating a statistical-experimental approach to identify testing variables of the SCB test that result in repeatable test results. Toward this end, five testing variables (the number of testing specimens, specimen thickness, notch length, loading rate, and testing temperature) of the SCB test were investigated due to their significant effects on mixture fracture characteristics. After statistical analysis of 18 specimens tested a typical testing variables, approximately, five to six specimens/replicates were found to be a reasonable sample size that could properly represent asphalt concrete fracture behavior

using the SCB test method. The coefficient of variation (COV) of the mixture fracture energy was used to evaluate the effect of each variable on the repeatability of test results. A range of 1 mm/min. to 5 mm/min. for the loading rate, a notch length from 5 mm to 25 mm, and a specimen thickness of 40 mm to 60 mm and a testing temperature of 15-40°C showed the lowest variation of fracture energy. The second part of this work is to investigate the sensitivity of the SCB test using the previously determined testing variables. Fourteen different asphalt concrete (AC) mixtures collected from 12 field construction projects in Nebraska were used in this task. The ANOVA test showed statistically significant differences between mixtures at a 95% confidence level. Tukey's HSD multiple-comparison analysis found similarities within mixtures of same types and significant difference between mixtures types. In addition, the fracture energy of bituminous mixtures increased with increasing amount of virgin asphalt content in mixture. Overall, the SCB test method developed herein proved to be repeatable and sensitive to changes in mixtures, and thus a promising tool for evaluating the fatigue fracture resistance of AC mixtures.

DEDICATION

To my beloved mother and my late father.

ACKNOWLEDGEMENT

I would like to thanks my adviser and committee member Yong-Rak Kim for the invaluable insights that opened my eyes on my research and academic life. He always gave me advice and encouragement and always believed in me. Thank you sincerely. God Bless him.

I would also like to thanks my committee members, Dr. Neghaban and Dr. Szerszen for their willingness to be on my committee and for providing advices that helped me advance my graduate career.

In addition, I would like to thank my research groupmates, Dr. Taesun You, Hesamaddin Nabizadeh, Hamzeh Haghshenas and Keyvan Zare Rami for advice throughout my program. I would also like to thanks Dr Im Soohyok for the training, advices and collaboration. I am also thankful for the peer reviews and comments from Karen Sterling and Brandon Riehl.

Most importantly, I am infinitely thankful for the support of my family, especially my mother. She has always been my inspiration and gave courage throughout my life. She gave me strength when I was weak and always believed in me. God bless her infinitely.

FINANCIAL SUPPORT

I would like to thank the Nebraska Department of Roads (NDOR) for the financial support that made this thesis possible.

TABLE OF CONTENTS

LIST OF FIGURES

LIST OF TABLES

CHAPTER 1 : INTRODUCTION

During its service life, asphalt concrete (AC) pavement is susceptible to several types of distresses, such as fatigue-cracking, rutting, and thermal cracking. Typically, the majority of these distresses are a result of repeated loading (fatigue) from traffic vehicles in combination with freezing and thawing cycles associated with temperature variations throughout the seasons of the year. The presence of these distresses directly and severely compromise the overall structural and functional performance of the pavement, and consequently diminish the service life and ride quality of roads. Damages become more accentuated when fatigue-cracking is combined with thermal stresses, resulting in potholes that render the pavement virtually unusable. In addition, in cases where the affected pavement is not rehabilitated in a timely manner, the distresses may provide easy access to moisture, resulting in the accelerated deterioration of pavement. This inevitably leads to increased repair costs that may strain the budget of a state's department of transportation (DOT). It becomes obvious that the pavement design process needs to take a combination of design factors that cause these undesired distresses into consideration, such as traffic loads, environmental effects, and material properties of AC mixture constituents, to increase reliability and service life of pavement.

Among the aforementioned AC pavement distresses, fatigue-cracking is the most critical in pavement considering that once it occurs, it may lead to rapid pavement structure deterioration and severely reduced ride quality. Thus, in order to mitigate this, it is imperative to explore and characterize the complex fracture mechanics behind crack initiation and propagation in AC mixtures and extract fracture parameters to serve in the

selection of better-suited mixtures to resist cracking/fracture.

Currently, the Superpave performance grade (PG) specification evaluates cracking behavior in asphalt concrete mixtures by only considering properties of asphalt cement. This method used the dynamic shear rheometer (DSR), bending beam rheometer (BBR), and direct tension test (DTT) developed by the Strategic Highway Research Program (SHRP). This approach, however, fails to consider the aggregate portion of the AC mixtures, which makes up about 90~95% of the total weight of the AC. SHRP attempted the indirect tensile test (IDT) creep and strength of AC performed according to AASHTO T322-07 (2007). The IDT is used to find critical cracking temperature parameters that are then employed in the thermal cracking (TC) prediction model implemented in the AASHTO Mechanistic-Empirical Pavement Design Guide (MEPDG). As a result of using the empirical model, the IDT cracking parameters fall short of properly characterizing crack initiation and propagation in AC mixtures, which are temperature, rate, and mode dependent (Im, Kim et al. 2013, Im, Ban et al. 2014). Similarly, the thermal model in AASHTO MEPDG fails to adequately address fatigue-cracking, which mainly occurs at intermediate temperatures (i.e., 15°C ~ 30°C).

Recently, the AC pavement community sought development of fracture mechanics-based tests in order to properly address the aforementioned issues. Test methods include the single-edge notched beam (SEB) test (Wagoner, Buttlar et al. 2005) and the disk-shaped compact tension (DCT) test (Marasteanu, Dai et al. 2002, Wagoner, Buttlar et al. 2005). Experimental tests in combination with a fracture mechanics model, such as a cohesive zone model (CZM), were attempted to better identify fracture characterization in AC (Song, Wagoner et al. 2008, Shen and Paulino 2011, Im, Ban et al. 2014, Im, Ban et al.

2014). The incorporation of a fracture mechanics model (e.g., cohesive zone model) into experimental tests is attractive in that it can be used to gain insights into the isolation of crack formation energy from other sources of energy consumption in fracture tests. In typical fracture tests of quasi-brittle materials, the total internal energy, which is a result of the external work done, is composed of several sources of energy: the recoverable strain energy, the energy dissipated by the fracture process, and the energy dissipated due to material inelasticity. Consequently, this approach permits researchers to obtain information from test results that were otherwise not feasible to obtain solely from laboratory tests. However, since CZM requires calibration for experimental test results, advances in laboratory fracture tests are needed in order to take full advantage of the approach. Among the several fracture test methods in AC mixtures, the semi-circular bend (SCB) test has gained increasing attention from the AC pavement community due to its efficient, repeatable, and practical ways to characterize asphalt concrete fracture behavior.

The SCB test results have shown sufficient testing sensitivities to testing variables such as loading rate, specimen thickness, and testing temperature (Allen, Lutif et al. 2009, Kim, Lutif et al. 2009, Li and Marasteanu 2009, Im, Kim et al. 2013). However, the selection of testing variables that can provide statistically representative fracture characteristics of asphalt mixtures has not been fully investigated. Thus, several studies (Li and Marasteanu 2009, Shu, Huang et al. 2010, Faruk, Hu et al. 2014) have performed SCB tests with testing variables selected somewhat randomly based on previous experiences/observations, which typically lead to inconsistent and non-repeatable fracture test results. In addition, it is not clear how many SCB specimens should be tested in order to examine the fracture behaviors of an asphalt concrete mixture. Obviously, it is necessary

to explore the SCB test with testing variables that can improve the repeatability and reliability of the fracture test results.

1.1 Research Objectives

The primary goal of this research is to investigate SCB testing variables so that the SCB test can be used in the form of a reliable-repeatable test method, particularly to evaluate the fatigue-cracking resistance of typical asphalt concrete mixtures. The specific objectives of this research are as follows:

1. To investigate the effect of individual SCB testing variables on asphalt concrete fracture behaviors at intermediate service temperatures.
2. To explore the SCB test method with testing variables that can provide reliable test results with statistical repeatability (consistency) and practicality.
3. To investigate the sensitivity of the SCB test method with different AC mixtures collected from field construction projects.

1.2 Research Methodology

To meet the objectives mentioned above, systematic testing efforts and statistical analyses were integrated to investigate core testing variables, such as the minimum recommended number of specimens for the SCB test, thickness of specimens, notch length, loading rate and the testing temperature. First of all, based on an extensive literature review of SCB test, reasonable testing variables were assumed. Using these variables, SCB testing results from a total of 18 specimens were used for a statistical analysis that estimated the required number of specimens necessary with a desired confidence level (i.e., 95%) and margin of

error (i.e., 0.05). This integrated experimental-statistical approach led to a recommended combination of the SCB testing variables to characterize the cracking resistance of asphalt concrete mixtures at intermediate service temperature conditions. With the minimum number of specimens investigated, the effect of each of four critical testing variables (thickness of specimens, notch length, loading rate, and temperature) was then explored by varying one variable at a time while others remained constant. This allowed to isolate and characterize the effect of each variable on test results. The consistency in the test results was evaluated by the coefficient of variation (COV) of fracture energies. The COV is defined as the standard deviation divided by the mean (Dowdy, Wearden et al. 2011). Test-analysis results would recommend ranges and values of testing variables that exhibited the least/acceptable variability of test results. Subsequently, using the recommended testing variables, the sensitivity to difference in AC mixtures was evaluated by testing 14 AC mixtures collected from 12 field construction projects in Nebraska. Field projects were chosen to be representative of all AC mixture types used in Nebraska. The research methodology employed in this study is summarized in Figure 1-1 below.

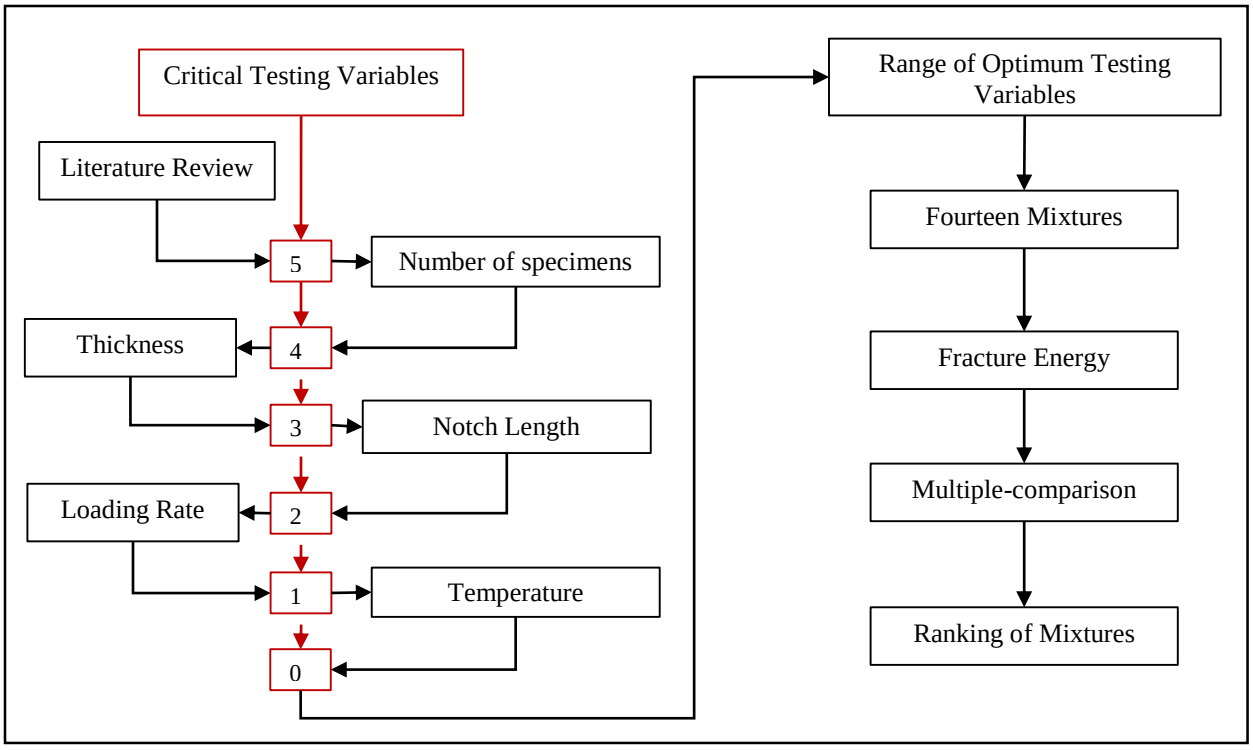

Figure 1-1 Research methodology used in this study

1.3 Organization of Thesis

This thesis is composed of six chapters. At the end of this introduction, Chapter 2 covers literature review on SCB test method as fracture testing method. Chapter 3, presents the material and testing facility used in this study. Chapter 4 include the process of determining the minimum number of specimens for SCB test and SCB test method development by considering the effect of critical test variables (i.e., specimen thickness, notch length, loading rate, and testing temperature) on fracture energy and on repeatability of the test results. Chapter 5 covers testing of 14 Nebraska plant-produced asphalt concrete mixtures collected from 12 separate field construction projects in Nebraska using the testing variables previously developed in Chapter 4. This chapter attempts to characterize the sensitivity of fracture parameters to changes in AC mixtures. Laboratory SCB test results

in a form of fracture energy (G_f) were statistically investigated for this purpose. Finally, Chapter 6 summarizes the main findings and conclusions of this study.

CHAPTER 2 : LITERATURE REVIEW

Toward achieving the main goals of this study, a literature review was conducted on existing methods of assessing fracture performance in asphalt concrete mixtures. This chapter includes key studies conducted on the subject matter and summarizes relevant findings. Accordingly, this chapter presents both experimental and analysis methods employed by other researchers toward characterization of asphalt concrete fracture behavior at intermediate testing temperatures, particularly those using the SCB test method.

2.1 Fracture Mechanics

Fracture mechanics is a useful tool destined to characterize crack initiation and propagation in materials. Fracture in notched materials occurs when the energy stored at the vicinity of a crack is equal to the energy required for the formation of new surfaces. It is noteworthy that this hypothesis requires a pre-existing crack/notch to be valid. Thus, most fracture test specimens include a pre-crack or notch. When the material at the vicinity of the crack (i.e., fracture process zone) relaxes, the strain energy is consumed as surface energy and the crack grows by an infinitesimal amount. If the rate of strain energy release is equal to the fracture toughness, then the crack growth takes place under steady-state conditions and the failure eventually occurs.

2.2 Fracture Characterization of Asphalt Concrete Mixtures

In an effort to characterize the fatigue-fracture in AC mixtures and, concurrently, to improve the mechanical and structural performance of AC pavement, various fracture

testing methods such as the single-edge notched beam (SEB) test (Figure 2-1 (a)), the disk-shaped compact tension (DCT) test (Figure 2-1 (b)), and semi-circular bending (SCB) test (Figure 2-1 (c)), have been attempted. It is noteworthy that tests herein explore mode I fracture in which the loading direction and the initial notch are directly aligned with the specimen's centerline. This set-up is to solely induce tensile stresses at the bottom of the specimen resulting in crack propagation.

The SEB test involves three point bending of a notched AC beam. SEB is advantageous to investigate pure mode I simple loading configuration and mixed mode testing by slightly moving the notch away from the centerline. This geometry, although it is attractive numerically, as demonstrated in several studies (Paulino, Song et al. 2004, Song, Paulino et al. 2005), is impaired by a complex specimen fabrication that requires significant testing efforts. In addition, this test is also not efficient for field cores that are usually circular disks while deep-notched laboratory specimens may result in crack initiation under self-weight (Wagoner, Buttlar et al. 2005).

Another test sought by researchers is the disk-shaped compact tension (DCT) test, shown in Figure 2-1(b). The DCT test has been standardized in the ASTM E399, "Standard Test Method for Plane–Strain Fracture Toughness of Metallic Materials." The specimen has a circular geometry with loading holes on each side of the notch. This geometry can maximize the fracture area and is thereby able to reduce the geometry-associated variability of test results. However, as mentioned by Wagoner, Buttlar et al. (2005), there is a possibility of stress concentration at the loading holes that can result in a premature specimen failure with an erroneous outcome. Moreover, specimen fabrication and preparation for the DCT test are not simple due to the accessories required to position the

specimen in the testing mount to induce pure opening mode fracture. The DCT test is further hampered by potential crack deviation from the center of the specimen during testing.

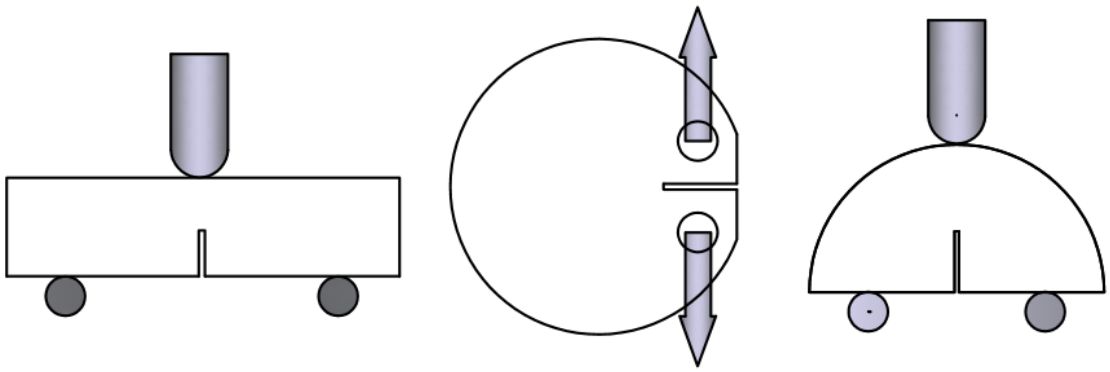

(a) (b) (c)

Figure 2-1 Fracture tests for asphalt concrete mixtures: (a) single-edge notched beam (SEB) test, (b) disk-shaped compact tension (DCT) test, and (c) semi-circular bending (SCB) test

Because of the issues of the aforementioned fracture tests, a semi-circular bending (SCB) test (Figure 2-1 (c)) has been attractive in the flexible (AC) pavement community. This test is used by many researchers, such as (Wu, Mohammad et al. 2005, Li and Marasteanu 2009, Shu, Huang et al. 2010, Liu 2011, Aragão and Kim 2012, Biligiri, Said et al. 2012, Zegeye, Le et al. 2012, Im, Kim et al. 2013, Kim and Aragão 2013, Im, Ban et al. 2014, Saadeh, Hakimelahi et al. 2014) due to its several advantages: (1) easiness and effectiveness in fabricating specimens, (2) suitability for field cores, and (3) repeatability in testing results (Wu, Mohammad et al. 2005, Li and Marasteanu 2009, Aragão and Kim 2012, Im, Kim et al. 2013, Im, Ban et al. 2014).

Initially, the SCB test method was proposed by Chong and Kuruppu (1984) because other existing fracture tests based on linear-elastic fracture mechanics (LEFM) were expensive and difficult to perform using rock materials. As seen in Figure 2-1(c), the SCB test method is fundamentally a three point bending test of a semi-circular shaped specimen with an introduced notch. This geometry induces tension at the bottom of the sample resulting in the crack propagation throughout the specimen. The SCB test has proven to be adequate for evaluating the fracture properties of both laboratory-compacted samples and field cores due to simplified specimen preparation (Huang, Shu et al. 2013). Although a specimen for the SCB test has a lower potential fracture area compared to one for the DCT test, the semi-circular geometry enables the testing of twice as many specimens obtained from field cores or laboratory-compacted samples compared to the DCT. In addition, the SCB has shown great potential for characterizing the mixed mode fracture behavior of asphalt mixtures by simply adjusting the inclination angle of the notch or the space between two supports (Im, Ban et al. 2014, Im, Ban et al. 2014).

Zegeye, Le et al. (2012) investigated the size effect fracture in asphalt mixtures at a low temperature using the SCB test. In this work, SCB specimens were prepared with four different diameters: 76.4 mm, 101 mm, 147 mm, and 296 mm. For every diameter size, specimens were notched to match a notch to radius (c/r) ratio of zero (notchless), 0.05, and 0.2. In this study, the testing temperature was -24°C. It was observed that large notchless specimens (i.e., 296mm in diameter and c/r = 0) crack always initiated far from the centerline where the measuring gauge was installed. It was also observed that the nominal strength of specimens decreased as the size of specimens increased. It was noted from this study that large specimen (larger than 150 mm in diameter) preparation is arduous

and less practical since most AC mixture compactors and field cores are 150 mm in diameter. This can explain the scarcity of studies that used specimens with large diameters in AC sample preparation.

Wu, Mohammad et al. (2005) evaluated fracture resistance in several Superpave AC mixtures with different binder contents and nominal maximum aggregate sizes (NMAS) using the SCB test. Specimens were prepared using a 3 mm wide saw at three different notch lengths: 25.4 mm, 31.8 mm, and 38 mm, with three replicated for each case. Specimens were monotonically loaded at load point displacement (LPD) rate of 0.5 mm/min at a temperature of 25±1°C. Statistical analysis of the test results illustrated that the peak load might be sensitive to the binder type, compaction level, or the NMAS at the notch length of 25.4 mm, and only sensitive to NMAS at a notch length of 31.8 mm. At notch length of 38.0 mm, the peak load was not sensitive to any of the variables. From this study, it was also found that the strain energy was only sensitive to the NMAS and only at the notch depth of 31.8mm. This study found that the SCB test was fairly sensitive to all mixture variables selected and that Superpave mixtures with larger NMAS exhibited better fracture resistance due to larger stone-to-stone contact. It was concluded that the SCB test method can be a valuable tool in the evaluation of the fracture resistance of AC mixtures.

Using the SCB test, Li and Marasteanu (2009) evaluated low temperature fracture resistance on AC mixtures with different aggregates (limestone and granite) and binder types: PG 58-28, PG 64-28, and a modified PG 64-28 SBS (Styrene Butadiene Styrene) compacted both at 4% and 7% air voids. Specimens used in this study were 25 mm thick with notches ranging from 5 mm to 30 mm in length, and width of 2 mm. The test was conducted at three temperatures: -6°C, -18°C, and -30°C, at a 0.0005 mm/sec crack mouth

opening displacement (CMOD) rate. It was found that higher air voids resulted in lower fracture resistance in terms of fracture energy. In addition, asphalt PG grade had an effect on fracture energy results with the mixtures with a high PG grade of 58 asphalt displaying higher fracture energy and the lowest peak load at -30°C. The general trend showed that fracture energy increased with temperature at 5 mm notch length in contrast to peak load. This effect was diluted at other remaining notch lengths.

Biligiri, Said et al. (2012) evaluated the crack propagation potential of AC mixtures with 4.4% and 5.4% asphalt (binder) contents using the SCB. The test was conducted at 10°C (the standard testing temperature for fatigue evaluation in Sweden) on 50 mm thick specimens with 15 mm long and 2 mm wide notches. The test was conducted at a 1 mm/min LPD loading rate and at three temperatures: -10°C, 0°C, and 10°C, with four replicates tested for each case. It was found that increasing the asphalt content, from 4.4% to 5.4%, reduced the mixture's fracture toughness, thereby decreasing its ability to resist higher traffic loads. Laboratory test results showed that mixtures with higher asphalt content significantly improved crack propagation resistance in terms of facture energy, while a higher resistance to fatigue-cracking and propagation was observed from field cores.

In 2012, Aragão and Kim (2012) conducted a numerical and experimental effort to characterize mode I fracture behavior of bituminous paving mixtures subjected to a wide range of loading rates at intermediate temperature conditions. In this study, a simple experimental protocol was developed using the SCB test geometry, and high-speed cameras with a digital image correlation (DIC) were incorporated to monitor local fracture behavior at the initial notch tip of the SCB specimens. The DIC results of the SCB fracture tests were then simulated using the finite element method, which was

incorporated with the material viscoelasticity and cohesive zone fracture model. As shown in

Figure 2-2, experimental results were successfully simulated using the numerical model. Furthermore, in Figure 2-3, the effect of the loading rate on fracture parameters was studied using the numerical model simulation. The results shows a clear dependency of fracture parameters (i.e., fracture energy and cohesive strength) to loading rates above 5mm/min.

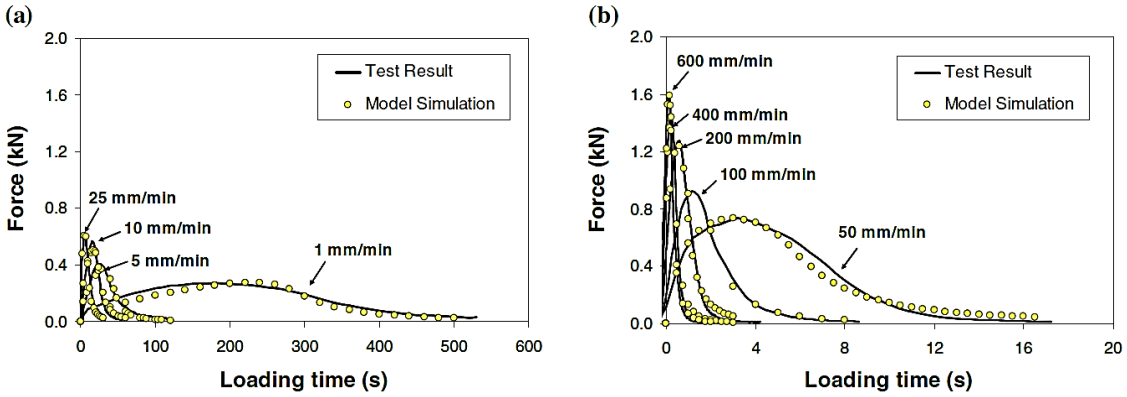

Figure 2-2 Effect of loading rate (Aragão and Kim 2012)

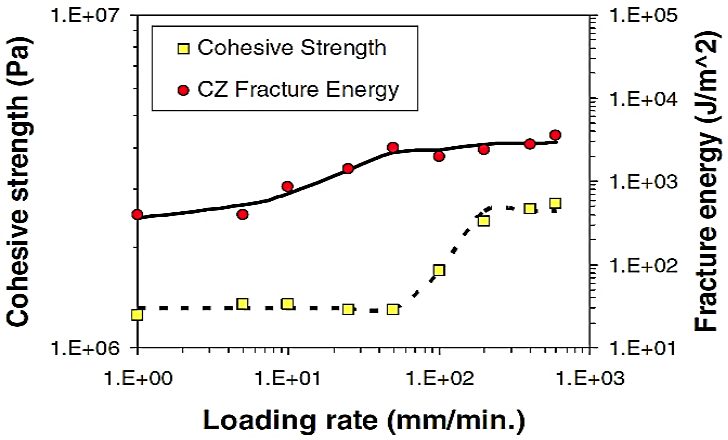

Figure 2-3 Numerical simulation results of SCB fracture testing at different loading rates (Aragão and Kim 2012)

2.2.1 Fracture Parameters

In both asphalt pavement research and the pavement community, fracture energy (G_f) has been used as a simple parameter representing fracture for AC mixtures. Generally, this property is less dependent on linear elasticity and homogeneity compared to other fracture properties, such as critical strain energy release rate and stress intensity factor (Marasteanu, Li et al. 2004). Thus, this method can be attractive for simply evaluating fracture

characteristics of an asphalt mixture that is highly heterogeneous and nonlinear inelastic. The fracture energy in Joule/m^2 is calculated by Eq. (2.1) (Marasteanu, Li et al. 2004):

$$G_f = \frac{W_o + mg\delta_o}{A_{lig}} \tag{2.1}$$

where W_o is fracture work, the area below the load-displacement curve, as shown in Figure 2-4(a). m is a mass, g is the gravitational acceleration, and δ_o is deformation. A_{lig} is the ligament area and can be calculated by:

$$A_{lig} = t(r - c) \tag{2.2}$$

where t is a thickness, r is a radius, and c is a notch length, as shown in Figure 2-4(b). It can be noted that the mass (m) of the specimen is negligible in Eq. (2.1) because small specimens are typically used, which infers an ignorable effect of specimen mass on the total fracture energy.

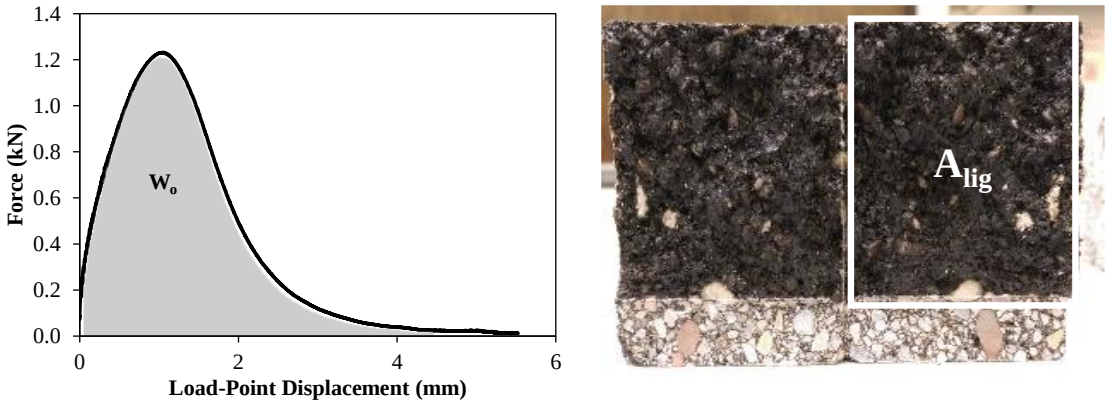

(a) (b)

Figure 2-4 Fracture energy (G_f) calculation: (a) fracture work (W_o) and (b) ligament area (A_{lig})

Considering a mode I type of fracture, in which the crack lies in a plane normal to the direction of largest tensile loading, the stress state around the crack tip is characterized using the stress intensity factor K_I (in N/mm$^{3/2}$) proportional to load P, and function of crack size (i.e., notch length) c and the geometry of the specimen. The stress value at any point near the crack tip is given by:

$$\frac{K_I}{\sigma_o\sqrt{\pi c}} = Y_{I(0.8)} \tag{2.3}$$

where, σ_o is the stress acting at a small distance (i.e., half span length *s*) and expressed as *P*/2*rt* with *P* being the load in MN. The geometric dimension of the specimen, *r*, *t*, and *c* are the radius, thickness, and notch length, respectively. The mode I normalized stress intensity factor $Y_{I(0.8)}$ is independent of size and load, but depends on the geometry of the specimen and the loading configuration. The span length used in this study (i.e., 120mm) and the 150mm diameter of the specimen result in a span ratio of 0.8 or,

$$Y_{I(120/150)} = Y_{I(0.8)} \tag{2.4}$$

and is expressed as calculated in (Lim, Johnston et al. 1993) by:

$$Y_{I(0.8)} = 4.782 + 1.219\left(\frac{c}{r}\right) + 0.063\times e^{\left(7.045\times\frac{c}{r}\right)} \tag{2.5}$$

(Lim, Johnston et al. 1993) approximated mode I stress intensity factors for various geometries of experimental interest using a finite element method based on the LEFM principles on rock materials.

The critical value of K_I for which failure occurs, referred to as fracture toughness K_{IC}, describes the local stress state that leads to the propagation of a crack. This stress

typically occurs at the highest load during testing, P_{max} (Figure 2-5). Therefore, K_{IC} represents the highest value of stress intensity factor that the material can bear without fracture (Zegeye, Le et al. 2012).

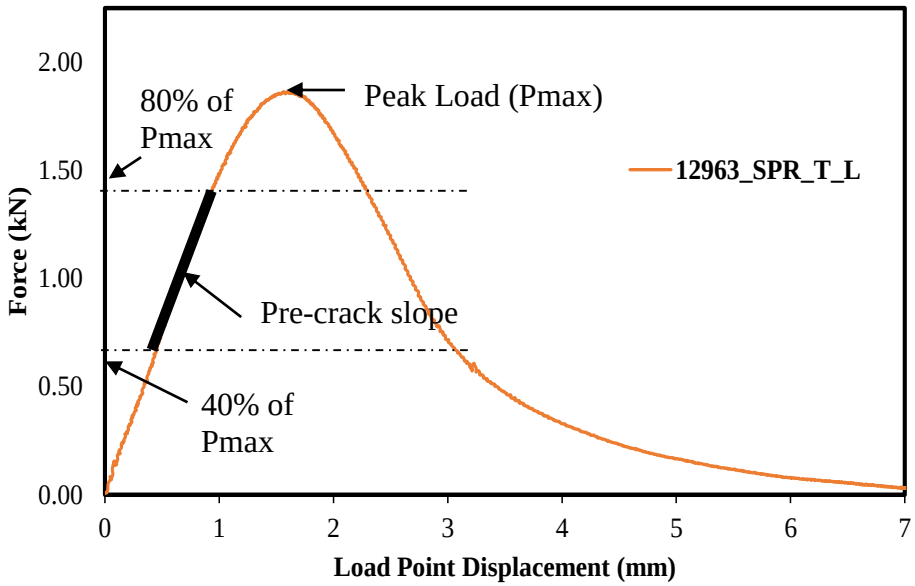

Figure 2-5 A typical force-LPD curve from SCB test

CHAPTER 3 : MATERIALS, TESTING FACILITY, AND SAMPLE FABRICATION

This chapter presents the materials and testing facility used to investigate effects of critical testing variables on repeatability of the SCB test results. The aggregate gradation, aggregate consensus properties, asphalt/binder content, and mixture design (i.e., air voids, binder content) of the AC mixture used in this task, are presented. Finally, the testing facility is also introduced.

3.1 Aggregate and AC Mixture

In this study, a typical Nebraska AC mixture (i.e., SPH) was used to prepare SCB specimens for laboratory tests. This mixture is typically used in Nebraska highways with a high traffic flow rate. As shown in Figure 3-1, it was collected during construction and brought back to the laboratory in sealed containers to prevent aging by oxidation. The mixture was then reheated for two hours in an oven to reach its recommended compaction temperature of 300°F. Subsequently, the mixture was compacted by a Superpave Gyratory Compactor (SGC) to target 4 ± 0.5% air voids.

The asphalt binder used in this study was Superpave performance graded PG 64-34 with a warm-mix asphalt (WMA) additive (Evotherm). By using a mixture from a single plant, a lengthy AC mixture preparation process was avoided and thereby reduced the inherent variations associated with the process. Proportionally, 5.20% of the asphalt cement (binder) content by the total weight of mixture and the 0.7% of WMA additive (Evotherm) by the weight of binder were mixed along with a blend of aggregates.

The aggregates were from four different sources; virgin aggregates, crushed gravel, 2A gravel, and reclaimed asphalt pavement (RAP), which were proportionally 10%, 50%, 5%, and 35% of the total weight aggregates. The whole aggregate blend had a nominal maximum aggregate size (NMAS) of 12.5 mm. It is noted that the presence of RAP in the mixture meant an addition of only 3.38% virgin binder to the blend of aggregates to reach the total binder content of 5.20%. This is due to the existence of asphalt cement in the old pavement millings (RAP).

Figure 3-1 Mixture collection from a dump truck at asphalt concrete plant

Table 3-1 presents aggregates gradation from the four different sources with their respective gradations. In addition, the bulk specific gravity (G_{sb}) and aggregate consensus properties (i.e., fine aggregate angularity [FAA], coarse aggregate angularity [CAA], flat and elongated [F&E] particles) of the final blend are also provided in the table.

Table 3-1 Gradation and consensus properties of aggregates used

Materials	**%**	**Sieve Analysis (Washed)**								
		3/4"	1/2"	3/8"	#4	#8	#16	#30	#50	#200
3/4" Clean	10	100.0	60.0	18.0	2.0	2.0	1.0	1.0	1.0	1.0
Crushed Gravel	50	100.0	100.0	100.0	92.7	73.0	45.2	29.1	16.2	6.3
2A Gravel	5	100.0	95.4	90.9	68.0	27.3	8.6	3.5	1.1	0.2
Millings (RAP)	35	100.0	94.2	93.2	85.1	52.3	38.4	25.1	19.8	7.8
Combined Gradation		100.0	93.7	89.0	79.7	56.4	36.6	23.6	15.2	6.0
Specification Range		–	90	–	–	28	–	–	–	2
		100	100	<90	–	58	–	–	–	10

Consensus Properties					
FAA	CAA	SE	F&E	D/B	Design G_{sb}
45	99/96	79	0.1	1.18	2.585

FAA: Fine aggregates angularity; CAA: Coarse aggregates angularity; SE: Sand equivalent; F&E: Flat and elongated particles; D/B: Dust to Binder Ratio; G_{sb}: Bulk specific gravity; – : Not Specified.

3.2 Testing Facility

During this study, all mechanical tests were conducted using the 25kN capacity Universal Testing Machine (UTM-25kN) equipment shown in Figure 3-2. This equipment is composed of an environmental chamber, a central data acquisition system (CDAS), and a hydraulic pressure system. It can produce a maximum of 25kN of static and 20kN of dynamic loading (at various frequencies). Additional information (i.e., key features and specifications) of the UTM-25kN test station are presented in Table 3-2. The environmental chamber can precisely control temperatures ranging from -16°C to 60°C. However, to ensure accurate temperature reading, a dummy AC sample with an internal thermometer was placed inside the chamber along with the SCB specimens to guarantee a target testing temperature, as shown in Figure 3-3.

Figure 3-2 UTM-25kN testing equipment

Table 3-2 UTM-25kN key specifications

Load Frame	
Size	185(H) × 58(D) × 60(W) cm
Weight	130kg
Load Capacity	25kN static, 20kN dynamic
Between Columns	45cm
Vertical Space	80cm
Stroke	50mm
Hydraulic Power Supply	
Size	81(H) × 40(D) × 70(W) cm
Weight	75kg (excluding oil)
Flow Rate	5litres/min
High Pressure	160 Bar
Low Pressure	2 to 160 Bar (adjustable)
Mains Power	208V / 230 V, 50 or 60 Hz, 2.6 kW
Noise Level	less than 70db at 2m

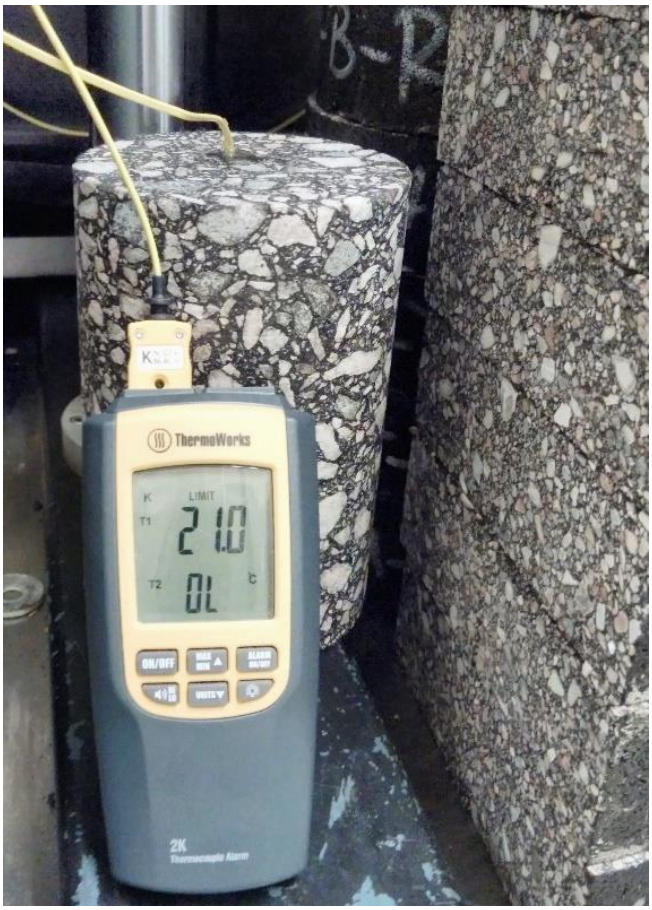

Figure 3-3 Reading temperature of specimens

3.3 Sample Fabrication and Test Set-up

As aforementioned, the AC loose (uncompacted) mixture (i.e., SPH) was reheated in an oven for two hours at 300°F (149°C). After ensuring this exact temperature with an infrared non-contact thermometer, the mixture was then compacted using the Superpave gyratory compactor (SGC) to produce tall compacted samples of 150 mm in diameter and 170 mm of height (Figure 3-4(a)), with a target air voids of 4 ± 0.5%. Multiple slices with various thicknesses, ranging from 30 mm to 60 mm in this study, were then prepared after removing the top and bottom parts from the tall compacted samples, as shown in Figure 3-4(b). Each slice was then cut into halves to yield two SCB specimens with a desired notch length of

two millimeters in width, as shown in Figure 3-4(c). It is noted that the introduced notch serves as crack initiator as this test is solely aimed at characterizing the fracture properties of AC mixtures during cracking propagation rather than by cracking initiation (European Committee for Standardization 2010).

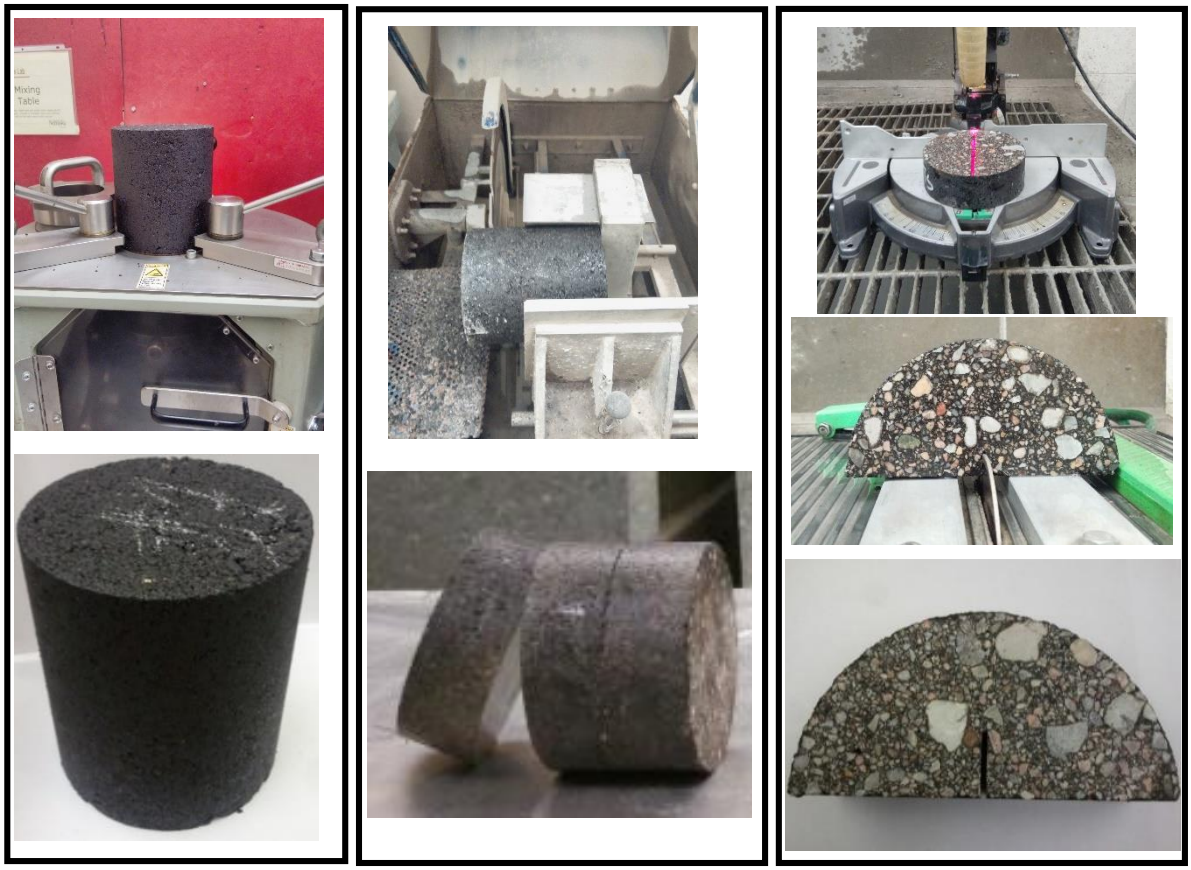

(a) (b) (c)

Figure 3-4 SCB specimen fabrication process: (a) compacting, (b) slicing, and (c) notching

For a more accurate test results analysis, the exact thicknesses and ligament lengths of SCB specimens were measured from three locations along the semi-circular edge and the results

were averaged, as shown in Figure 3-5. Afterward, specimens were placed inside the environmental chamber of the UTM-25kN and allowed a minimum of four hours to reach temperature equilibrium prior to testing. Subsequently, specimens were placed on a three point bending test fixture inside the environmental chamber to perform the test. The fixture has two cylindrical supports of 25 mm in diameter at each end, separated by a 120 mm span length. It is noteworthy that lubrication was applied to these supports to mitigate friction during testing.

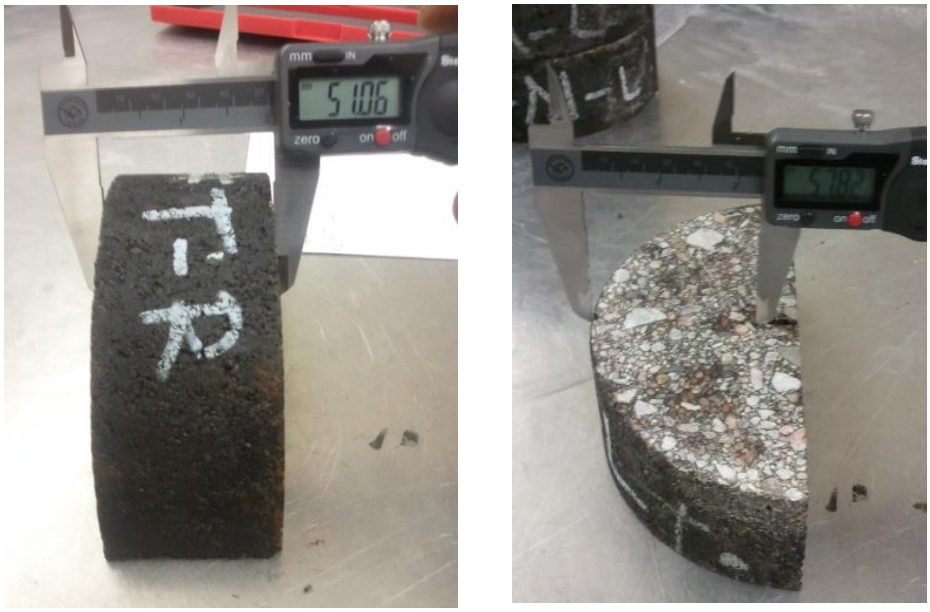

Figure 3-5 Recording the thickness and ligament length of SCB specimen

The device in Figure 3-6(a) was used to place specimens on the bending fixture in order to avoid eccentric loading. Then, a monotonic displacement rate was applied to the top center line of the specimen. A data acquisition system simultaneously monitored both the reaction force and the LPD during testing (Figure 3-6(b)). It is noted that each time, prior to testing, a small contact force of 0.10 kN was applied to the specimen.

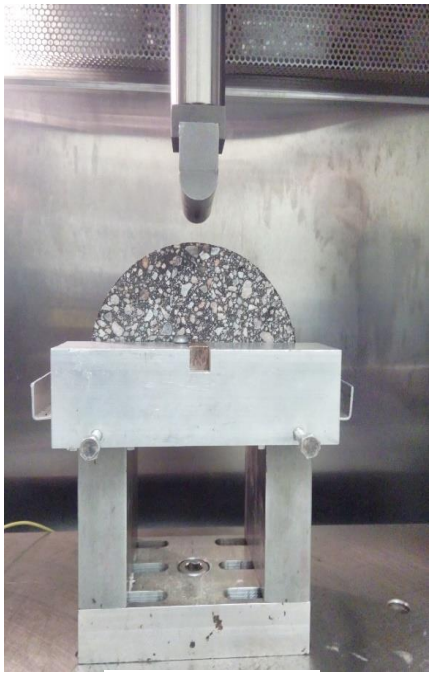

(a)

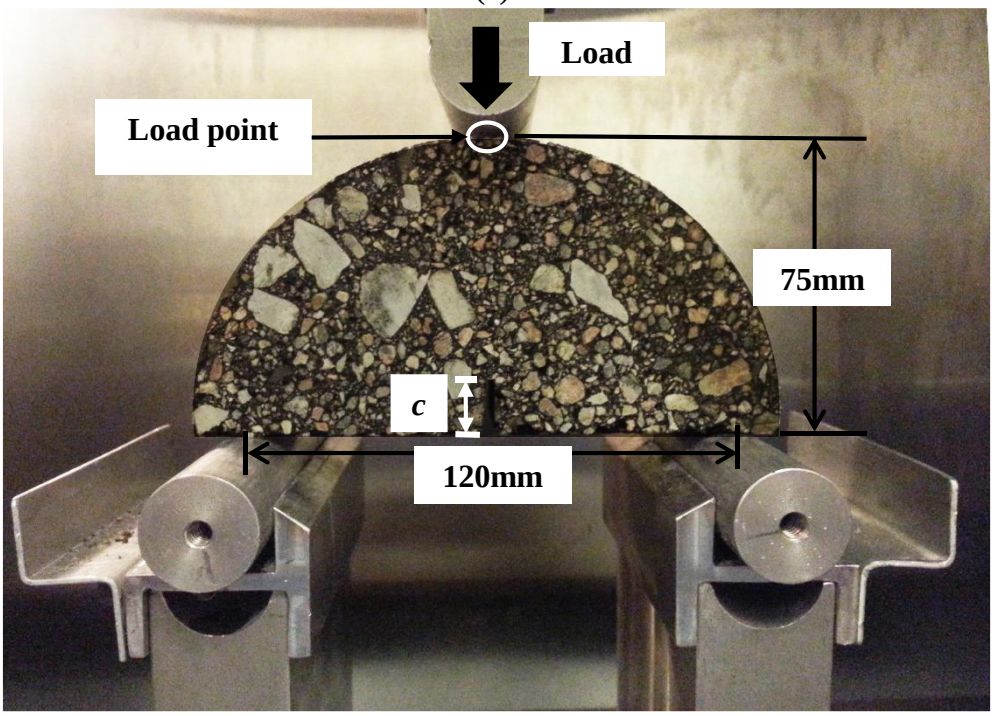

(b)

Figure 3-6 Test set-up for semi-circular bending (SCB): (a) specimen alignment before testing, (b) specimen ready to be tested

CHAPTER 4 : SCB TEST METHOD DEVELOPMENT

4.1 The Number of Testing Specimens

The number of specimens (sample size) of an experimental test is very critical in that; too large of a sample size may waste time and resources, while too small of a sample size may lead to inaccurate results. Therefore, determining the recommended minimum number of specimens for a test method is a significant task for reliable outcomes with high repeatability and efficiency. Consequently, the first effort the SCB test development was to statistically investigate the relationship between the sample size and the variation of the results.

Typically, the required sample size can be calculated by Dowdy, Wearden et al. (2011)

$$Z_{\alpha/2} = \frac{\bar{y} - \mu}{\sigma / \sqrt{n}} \quad \Rightarrow \quad n = \left[\frac{z_{\alpha/2} \times \sigma}{E} \right]^2 \tag{3.1}$$

where n is the number of specimens, Z is the standard normal deviate, σ is standard deviation of population, and E is the margin of error expressed as:

$$E = \bar{y} - \mu$$

where $\bar{y}$ is observed sample mean and μ is the true value of the population mean. Since the true population mean (μ) is often unknown, the margin of error (E) is usually introduced to achieve a desired accuracy. In this study, with a margin of error of 0.05 (E) and a confidence level of 95% (i.e., $Z_{\alpha/2} = Z_{0.025} = 1.96$), were used.

Eq. (3.1) can then be rewritten as:

$$n = \left[\frac{1.96 \times \sigma}{0.05}\right]^2 = 1536.64 \times \sigma^2 \quad (3.2)$$

Similar for the true population mean, the standard deviation of the population is often unknown. So in this study, the standard deviation (σ) of fracture energy of the population was rationally estimated after testing 18 SCB specimens and examining the relationship between population and standard deviation. This approach permitted a more accurate analysis to find *n*. The specimens were tested using typical SCB testing variables from the literature reviews such as: thickness of specimen = 50 mm (Duan, Hu et al. 2003), temperature = 21° C (Kim and Aragão 2013, Im, Ban et al. 2014), notch length = 15 mm ((Li and Marasteanu 2009, European Committee for Standardization 2010), loading rate = 1 mm/min. ((Biligiri, Said et al. 2012, Im, Kim et al. 2013).

Because the Eq.(3.2) was based on the assumption that the population (i.e., 18 SCB fracture energies in this study) came from a normal distribution, the normality of the test results should be checked prior to further analysis. As shown in Figure 4-1, the Lilliefors test (Razali and Wah 2011, Machiwal and Jha 2012) was conducted to compare the observed results to the expected results (i.e., normal distribution) of the same mean and standard deviation. The figure shows a good visual agreement between the expected fracture energy (i.e., the normal distribution) and the measured fracture energy. For a more quantitative normality check, a chi-square goodness-of-fit test was performed to check if the two distributions were statistically different at 5% significance level. The chi-square test resulted in the observed chi-square value (0.016) less than the critical value (27.587),

which demonstrates that the fracture energies of the 18 SCB specimens originated from a normal distribution.

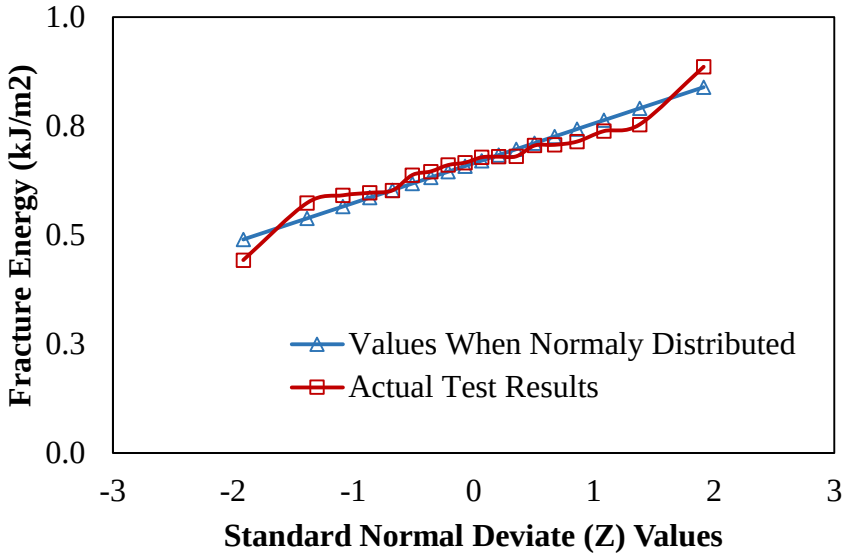

Figure 4-1 Normality test result.

As seen in Eq.(3.2), the number of specimens can then be determined by the standard deviation (σ) of fracture energy from an assumed population size. To find the relationship between the standard deviation of the population and the assumed population size ($k = 1, 2, \ldots, 18$ in this case), the number of all possible combinations (C_k^p) from the total count ($p = 18$) were calculated by:

$$C_k^p = \frac{p!}{k!(p-k)!} \quad \text{where } p=18 \text{ and } k=1, 2, 3, \ldots, 18 \tag{3.3}$$

Subsequently, corresponding standard deviations for each assumed population size (k) were obtained by averaging the standard deviations from the all possible combinations (C_k^p). Figure 4-2 (a) shows an example for the assumed population size (k) of five. Each

standard deviation of fracture energy for 8,568 combinations was calculated and used to obtain the average of standard deviation for $k = 5$.

Overall results of this process are presented in Figure 4-2(b). It is observed from the figure that there was a strong dependency of standard deviation on the assumed population size (k) of one to eight, followed by a steady saturation. Sequentially, Eq.(3.2) was used to calculate the minimum number of specimens (n) for each population size (k) assumed, and results are presented in Figure 4-2(c). It shows that the minimum number of specimens increased with increasing population size, and then tended to saturate at $n = 5\sim6$. Thus it can be inferred from this graph that five to six SCB specimens would be a reasonable sample size that can sufficiently represent the AC fracture behavior of the entire population (18 specimens in this case) with a 95% level of confidence. It should be also noted that the statistical analysis performed herein is reasonable because the minimum number of specimens (n) was always less than the corresponding population size (k), as shown in in Figure 4-2(c) (i.e., $n < k$).

Assumed Population Size of Five Specimens										
Specimen Name					Associated Fracture Energy (kJ/m^2)					Std. Dev.
1	2	3	4	5	0.442937	0.70566	0.886217	0.666351	0.754043	0.161587146
1	2	3	4	6	0.442937	0.70566	0.886217	0.666351	0.707196	0.158346526
1	2	3	4	7	0.442937	0.70566	0.886217	0.666351	0.574108	0.164066
		⋮					⋮			⋮
3	4	5	8	18	0.886217	0.666351	0.754043	0.66089	0.597246	0.111780105
3	4	5	9	10	0.886217	0.666351	0.754043	0.678727	0.602719	0.108506854
3	4	5	9	11	0.886217	0.666351	0.754043	0.678727	0.680773	0.092240535
		⋮					⋮			⋮
13	14	16	17	18	0.591544	0.714668	0.637955	0.679975	0.597246	0.053061009
13	15	16	17	18	0.591544	0.738708	0.637955	0.679975	0.597246	0.061458385
14	15	16	17	18	0.714668	0.738708	0.637955	0.679975	0.597246	0.057154921
Average of Standard Deviation										**0.083539845**

(a)

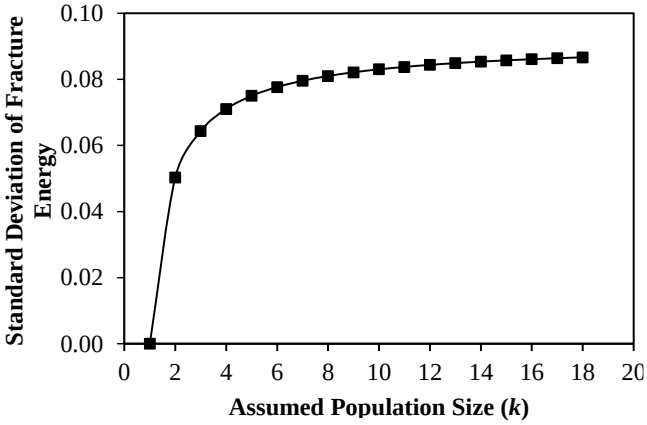

(b)

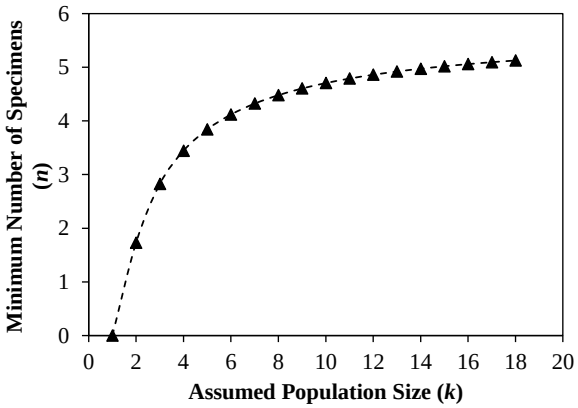

(c)

Figure 4-2 (a) Calculation of average standard deviation for k=5, (b) average standard deviation for each assumed population size (k), and (c) assumed population size (k) with associated

4.2 Specimen Thickness

Although previous studies (Brühwiler, Wang et al. 1990, Duan, Hu et al. 2003) highlighted that the thickness of specimens strongly affected fracture energy (G_f), less emphasis was placed on the effect of specimen thickness on testing repeatability. In this study, the fracture energy and variability of the test results for various thicknesses of specimens were investigated. As shown in Figure 4-3, the thicknesses varied from 30 mm, 40 mm, and 50 mm, to 60 mm. Other testing variables were reasonably selected based on literature reviews: temperature = 21° C (Kim and Aragão 2013, Im, Ban et al. 2014), notch length = 15 mm (Li and Marasteanu 2009, European Committee for Standardization 2010), loading rate = 1 mm/min. (Biligiri, Said et al. 2012, Im, Kim et al. 2013), and the number of specimens = six (Romero and Masad 2001). Figure 4-4 (a) shows that the peak force (P_{max}) increased as specimens became thicker. Additionally, the fracture energy increased from 30 mm to 50 mm, followed by a slight decrease at a thickness of 60 mm, as presented in Figure 4-4 (b). However, the fracture energy did not seem to be significantly dependent on the thickness of specimens within the thickness range tested. It is noteworthy that the results, in all cases, are an average of the six replicates.

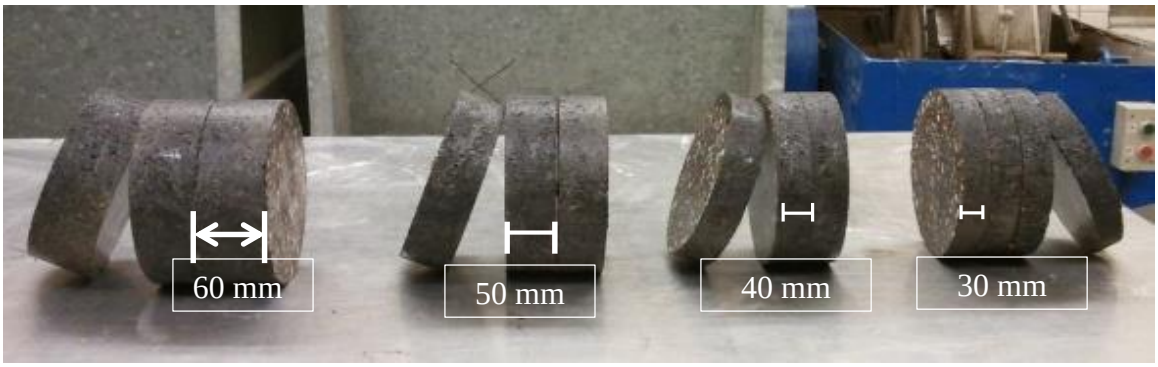

Figure 4-3 Fabrication of SCB specimens at different thicknesses

To evaluate the consistency of the testing results, the coefficient of variation (COV) of the fracture energy of each thickness was estimated. Figure 4-4(b) indicates a general decrease in COV with increasing thickness, while a steep decline between 30 mm and 40 mm was observed. This figure implies that a SCB specimen thicker than 40-50 mm is appropriate for characterizing the fracture behavior of AC without significantly increasing the variability of results when other variables are maintained. This finding agrees well with previous studies (Brühwiler, Wang et al. 1990, Wittmann and Zhong 1996), indicating that the thickness of AC specimens should be at least four times larger (i.e., 12.5 mm $\times 4 = 50$ mm) than NMAS size (12.5 mm in this study). For the subsequent steps, 50 mm was chosen based on other studies and the low COV ($\leq 10\%$) value found in this study.

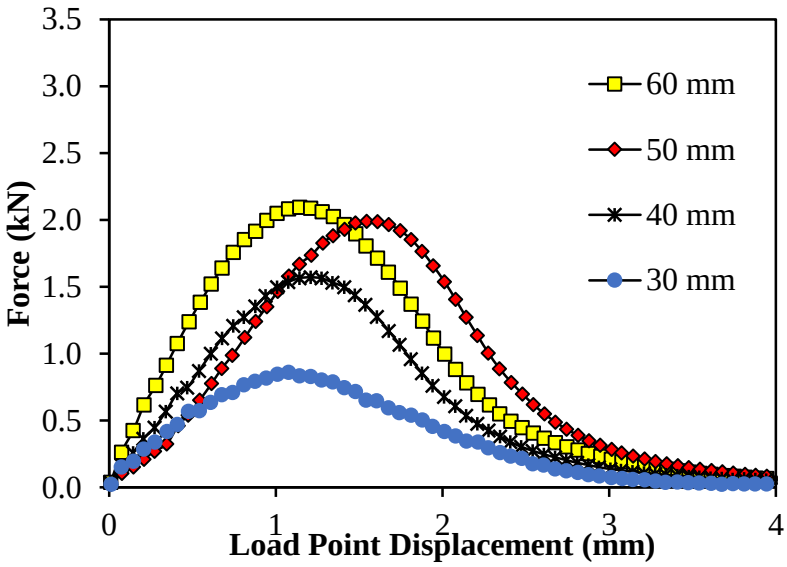

(a)

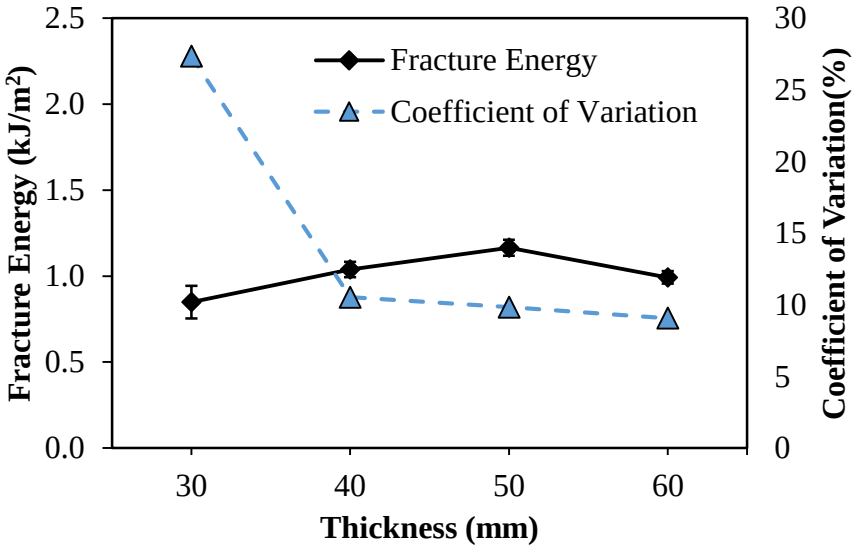

(b)

Figure 4-4 Effect of thickness of specimens (t): (a) test results (average of six replicates) and (b) fracture energy with standard error bars and COV of fracture energy for different thicknesses

4.3 Notch Length

To investigate the effect of notch length, specimens with five notch lengths (0 mm, 5 mm, 15 mm, 25 mm, and 40 mm) were tested. Other testing variables were fixed: the thickness of a specimen = 50 mm, loading rate = 1 mm/min, temperature = 21° C, and the number of specimens = six. Figure 4-5 (a) shows that the peak force and initial stiffness increased as notch length decreased. This trend is reasonable because specimens with smaller notch lengths have greater areas to be fractured, requiring more energy to fracture them. Another interesting observation from the figure is that the displacement at the peak force increases (i.e., shifts to the right) with decreasing notch length. Figure 4-5 (b) shows a decreasing trend of fracture energy along with increasing notch length. The fracture energy drops from around 2 kJ/m^2 in the case of the notchless specimens (i.e., 0 mm notch length) to around 0.5 kJ/m^2 for the specimens with 40 mm notch length.

The figure also presents the COV of fracture energy at various notch lengths. Due to the more random crack initiation/propagation, notchless specimens showed a higher COV than other specimens with a notch. Additionally, the high COV of the specimens with the longest notch length (i.e., 40 mm) might be explained by an insufficient ligament area (35 mm by 50 mm), which seems smaller than the typical size of a representative volume element (RVE). It is noted that a RVE is the smallest size of a specimen that should be tested in order to avoid a certain localized phenomenon and to provide a representative global response. Determination of the RVE size of a specimen is beyond the scope of this study. However, it can be noted from several previous studies that the RVE size of typical AC mixtures with a NMAS of 12.5 mm is around 60 mm by 60 mm (Romero and Masad 2001, Kim, Lutif et al. 2009, Kim, Lee et al. 2010).

Figure 4-5 (b) shows that a COV value of less than 10% can be achieved from specimens with notch lengths between 5 mm and 25 mm.

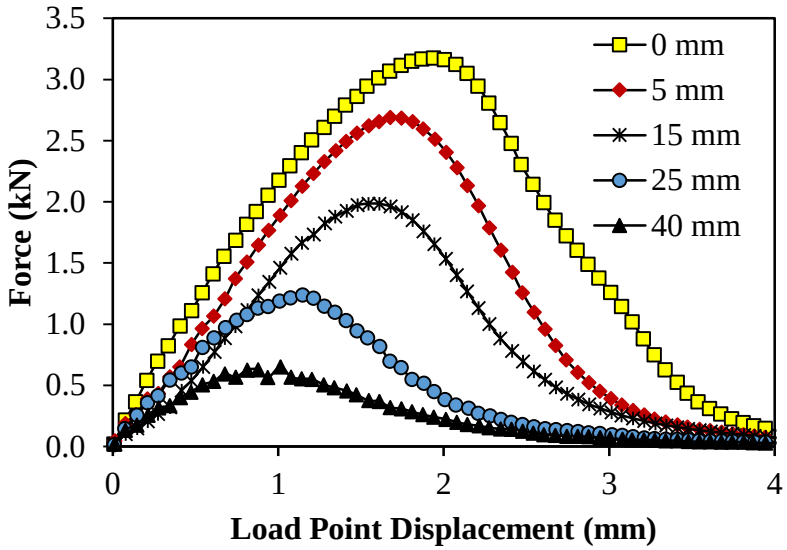

(a)

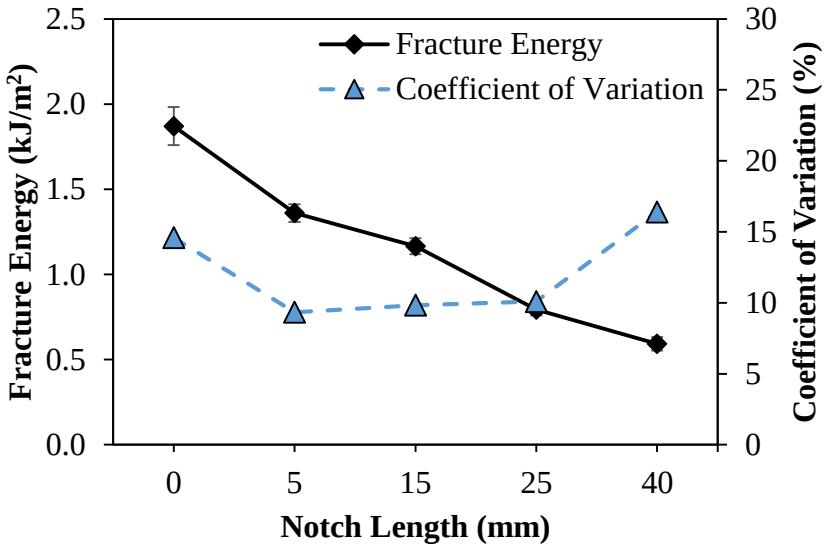

(b)

Figure 4-5 Effect of notch length: (a) test results (average of six replicates) and (b) fracture energy with standard error bars and COV of fracture energy for different notch lengths

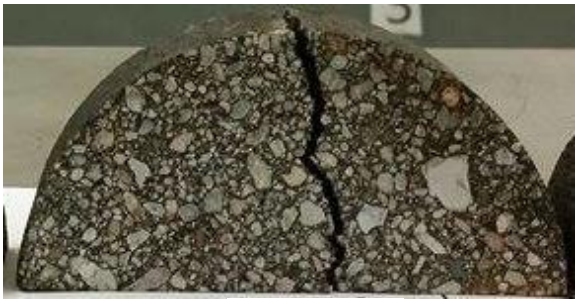

0 mm

5 mm

15 mm

25 mm

Figure 4-6 Fracture profile at different notch lengths

Although a 5 mm notch specimens presented the lowest COV within the range on notch lengths investigated in here, the resulting crack propagation deviated highly from the centerline of the specimen to be considered mode I fracture (see Figure 4-6). Consequently, a 15 mm notch was chosen to be used in the next step due to the relatively better cracking propagation profile and the repeatability of the test results.

4.4 Loading Rate

The loading rate has strong effects on the fracture behavior of AC mixtures under intermediate temperature conditions because of the viscoelastic deformation characteristics of asphaltic materials, as demonstrated by many studies including (Kim and Aragão 2013, Im, Ban et al. 2014). In this study, SCB specimens were tested at five different loading

rates: 0.1, 0.5, 1.0, 5.0, and 10 mm/min (Figure 4-7). Other testing variables remained constant (i.e., thickness of a specimen = 50 mm, notch length = 15 mm, temperature = 21° C, and the number of testing specimens = 6).

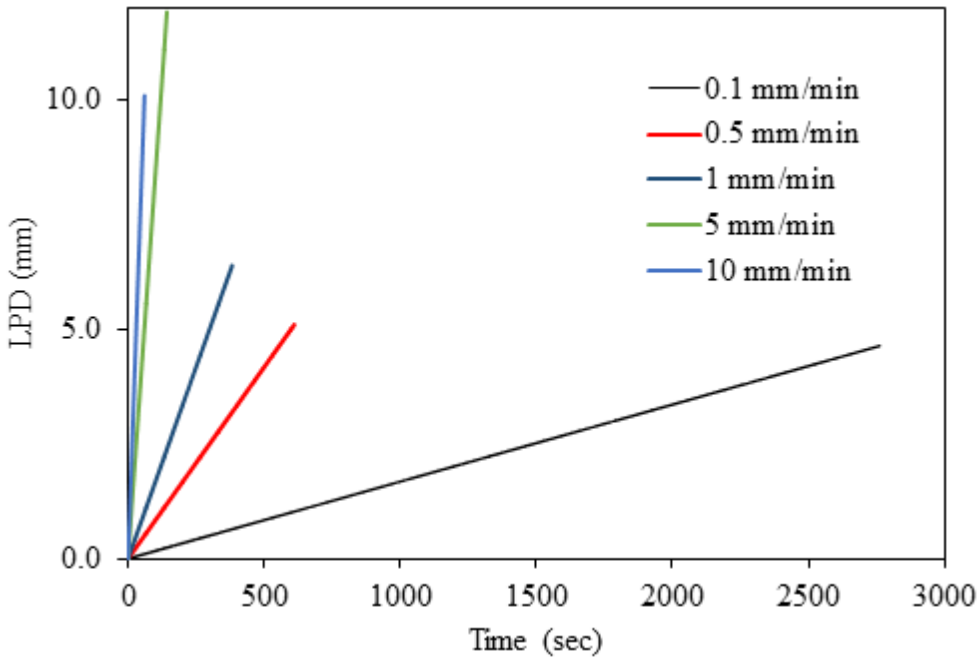

Figure 4-7 Loading rates inputs

The experimental results in Figure 4-8 (a) indicated that AC mixtures at slower loading rates showed more compliant responses, while the mixtures exhibited stiffer responses with greater peak force at faster loading rates. This observation agrees with findings from previous studies (Im, Kim et al. 2013, Kim and Aragão 2013, Im, Ban et al. 2014).

Although loading rates greatly influence AC force-displacement behavior, as shown in Figure 4-8 (b), the fracture energy was not significantly affected by the loading rate within the range tested in this study. It is noted that the fracture energy between one to five mm/min. stayed constant. In addition, compared to other testing variables, such as the

thicknesses of specimens and notch lengths (see Figure 4-4 (b) and Figure 4-5 (b)), low COV values were observed in all cases tested with a range between 0.1 mm/min. and 10 mm/min. Although the loading rates from 0.1 mm/min. to 0.5 mm/min. showed the lowest COV values, it is important to mention that testing at this rate is lengthy (3,000 sec. and 600 sec. for 0.1 and 0.5 mm/min, respectively) while providing no significant improvement to repeatability of test results compared to other loading rates evaluated herein. If one selects a threshold COV of 15%, any loading rate within the range can be chosen for the SCB test. Thus for the next step (i.e., investigation of testing temperature), a loading rate of 5 mm/min. was selected based on practicality.

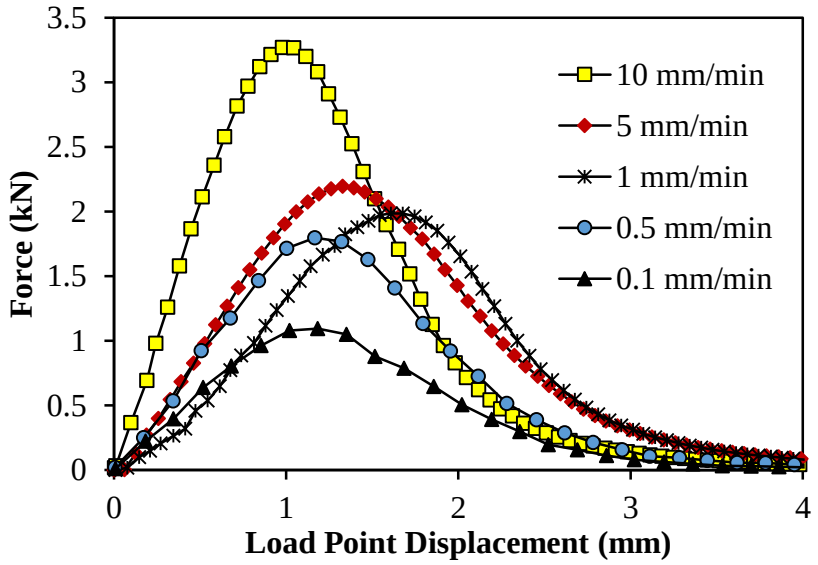

(a)

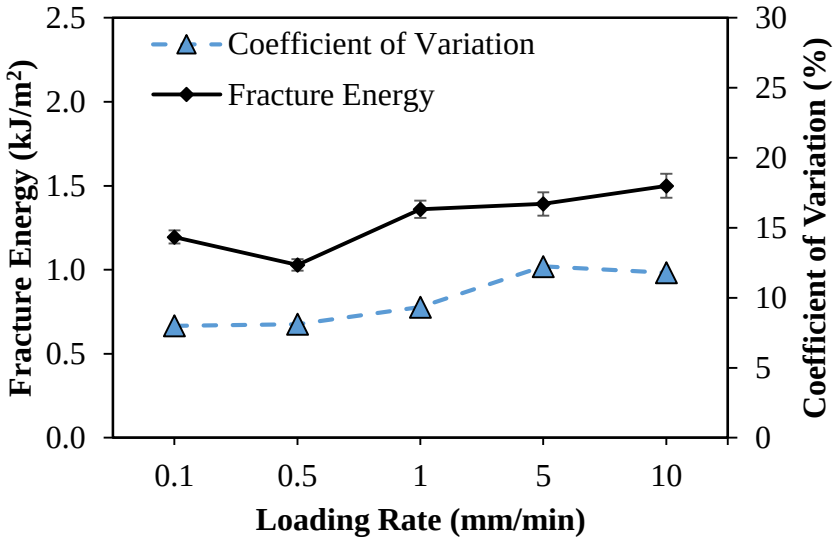

(b)

Figure 4-8 Effect of loading rate: (a) test results (average of six replicates) and (b) fracture energy with standard error bars and COV of fracture energy for different loading rates

4.5 Testing Temperature

It is widely documented that AC is highly temperature-dependent due to the viscoelastic nature of asphalt cement (Marasteanu, Li et al. 2004, Im, Kim et al. 2013). Based on this, the next step was to characterize the temperature effect on the repeatability of the test results, particularly for characterizing the fatigue-type cracking potential of mixtures. As shown in Figure 4-9, three different temperatures: 15, 21, and 40°C, were attempted to investigate their effects on fracture energy.

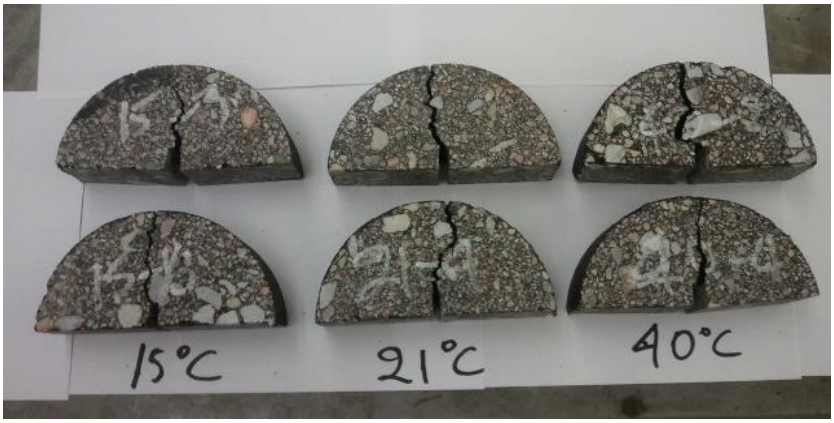

Front

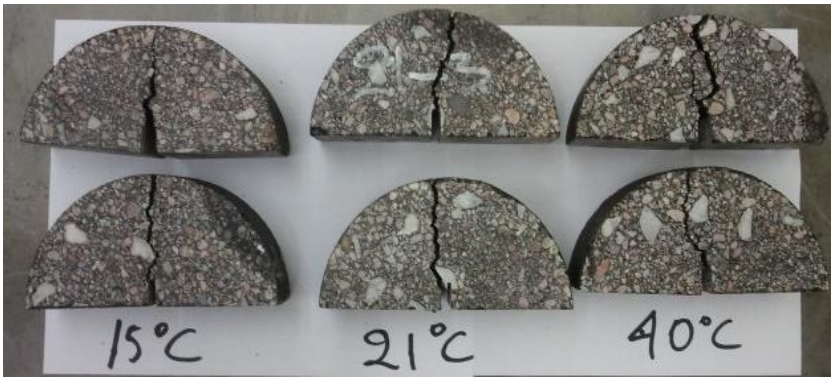

Back

Figure 4-9 Fracture profiles at different testing temperatures (front and back)

Other testing variables were used as such: thickness of specimens = 50 mm, notch length = 15 mm, loading rate = 5 mm/min., and the number of specimens = 6. The figure clearly shows that peak force and fracture energy were inversely proportional to testing temperature, which contrasts with the findings when the test was performed at low temperatures (e.g., below 0°C) (Wagoner, Buttlar et al. 2005, Li and Marasteanu 2009).

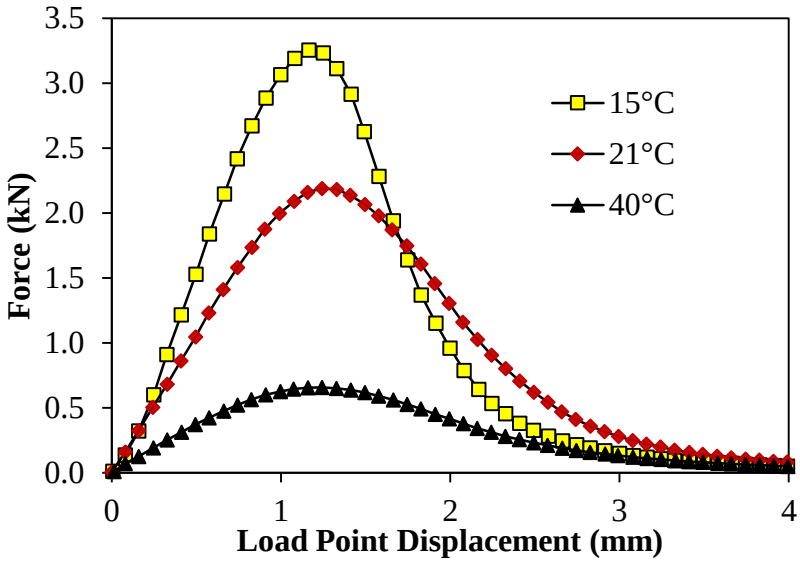

(a)

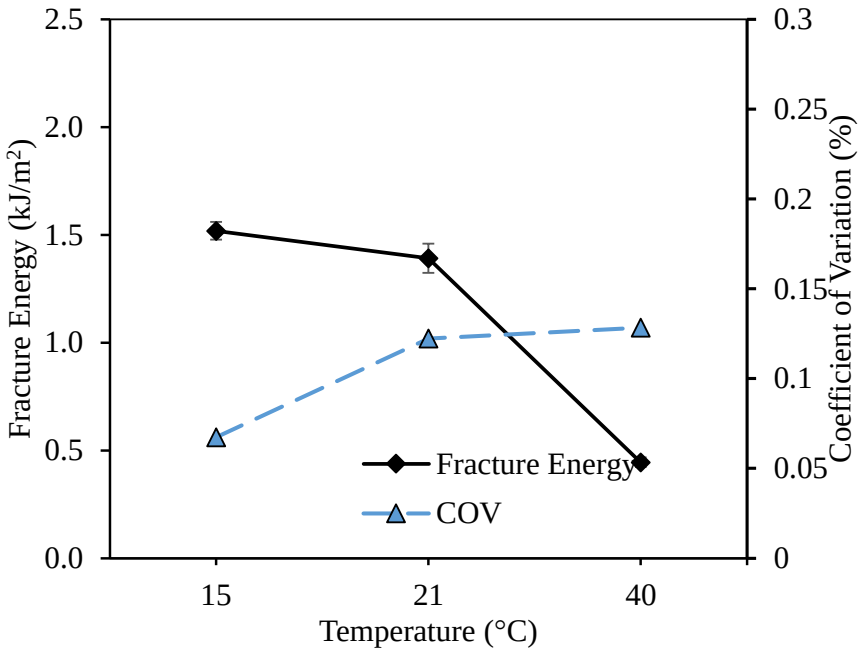

(b)

Figure 4-10 Effect of temperature: (a) test results (average of six replicates) and (b) fracture energy with standard error bars and COV for different testing temperatures

Figure 4-10 (b) presents the COV of fracture energy at different temperatures. As shown, lower temperatures presented smaller testing variations, with specimens at 15°C showing the lowest COV value of less than 10% in this study. Nonetheless, it can be noted that SCB testing at 21°C temperature could be quite attractive, with only a little loss of testing repeatability, when one considers the practical applications of the SCB test method for engineering purposes. This is because 21°C is a room temperature that is easily achievable without a sophisticated environmental chamber for testing equipment, and is a reasonable temperature that can properly represent fatigue-type cracking events.

4.6 Summary of SCB test method development

After determining the minimum recommended number of specimens and investigating the effect of each critical variables on repeatability of the test results, the range of test variables can be recommended when conducting SCB test (see Table 4-1). It is noteworthy that the COV of test results in terms of fracture energy from variables selected within this range should be less or approximately equal to 15%.

Table 4-1 Recommended variables for SCB test with approximate associated COV.

Test Variable	**Recommended Values**
Thickness (mm)	40~50
Notch Length (mm)	5~15
Loading Rate (mm/min.)	1~5
Temperature (°C)	15~40
No. of Specimens	5~6
COV (%)	**≤ 15**

CHAPTER 5 : SCB TESTING OF NEBRASKA PLANT-PRODUCED MIXTURES

In this chapter, the sensitivity of the developed SCB testing method was investigated through a field program. Fourteen AC mixtures collected from 12 different field construction projects (see Table 5-1) were tested. Mixture performance was ranked according to the fracture energy resulting from the SCB fracture test method. Statistical analyses were then conducted to investigate the sensitivity of the SCB test method to changes in AC mixtures.

5.1 Project Selection

Field projects were selected considering type of mixture, location of project, and availability of other important information such as pavement structure configuration, traffic and weather information, rehabilitation history of the pavement, etc. It is noteworthy that the accessibility to mixtures collected in a timely manner was also a decisive factor in selecting field projects. Since the main objective of this task is to test the sensitivity of the SCB test from different types of Nebraska AC mixtures and ultimately correlate the SCB test results with field cracking performance, it was important to collect other relevant information that is critical to conducting validation with actual field cracking performance. In this way, the laboratory SCB test results can be properly correlated to the field performance of the same mixtures over their service life. The field performance would be recorded through a routine Nebraska Pavement Management System (PMS).

Based on the selection criteria above, a total of 14 AC mixtures were collected as representatives of all different types of AC used in Nebraska. These mixture were collected

from 12 separate field construction projects, as shown in Table 5-1. In this table, detailed information about the construction projects, control number, highway name, thickness of the AC layer constructed, and specific project location are given.

Table 5-1 Field project selected for this study

Mixture Type	Control Number (CN)	Highway	Fill (inch)	Location
SPH	42515	80	2	Henderson to Waco
	22586	80	2	50th St. - I-480, Omaha
	42514	80	2	Hampton to Henderson
SRM	42567	281	4	St. Paul North
SLX	M4TLOB	4	1	Lawrence East
	M1041	41	1	N-41, US-77-Adams & US-77 Truck Scales
	M4TLOA	56	1	Hwy 91 - Spaulding East & West & HWY 56
SPR	12963	63	4	US-34-Alvo
	22454	91	4	Blair West
	12980	92	4	Brainard East & West
	42399	30	4	Wood river - Grand Island
	42567	281	3.5	Saint Paul north
SPS	42399	30	2	Wood River to Grand Island
	42514	80	2	Hampton to Henderson

Note: HWY: Highway

5.2 Material Collection and Sample Fabrication

All materials were collected from the mixture production plants prior to paving and were transported in a sealed container to minimize mixture aging. Figure 5-1(a) exemplifies a field construction in progress at highway 63 where the SPR_12963 (SPR with control number of 12963) mixture was collected. Figure 5-1 (b) presents mixtures after the compaction process. All mixtures were heated up to their respective specified compaction temperatures, as shown in Table 5-2, and then compacted to a target air voids of 4 ± 0.5%

(a) (b)

by the Superpave gyratory compactor (SGC).

Figure 5-1 Field program: (a) construction in progress on highway 63 (CN: 12963), (b) after laboratory compaction of mixtures

Table 5-2 Compaction temperature for each mixture

Mixture Type	Control Number (CN)	Comp. Temp. (ºF)
SPH	42515	300
	22586	300
	42514	290
SRM	42567	290
SLX	M4TLOB	285
	M1041	285
	M4TLOA	285
SPR	12963	280
	22454	290
	12980	290
	42399	290
	42567	290
SPS	42399	280
	42514	280

5.2.1 Aggregates Gradation

Aggregates gradation of five representative AC mixtures (one per each type of mixture) are shown in Figure 5-2. As seen in the figure, with the exception of SLX and SPS, all mixtures have a portion of coarse aggregates that can be associated to their functional aspect. For instance, SLX is usually used for thin-lift overlay pavement preservation AC layer that is typically one-inch in thickness, while the SRM is a base mixture typically used

to replace a hydrated lime slurry stabilized base and/or cold foam reclamation layer. Thus, SRM contains a higher percentage of coarse aggregates compared to SLX and/or SPH. This observation is also apparent in the visual microstructures of SCB specimens, as shown in Figure 5-3.

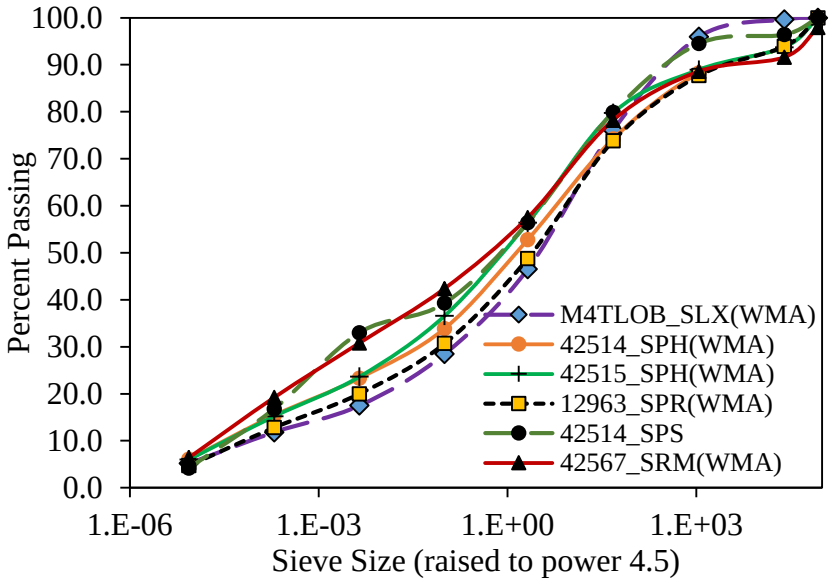

Figure 5-2 Gradation chart of five representative mixtures – sieve sizes raised to 0.45 power

42514_SPH

M4TLOB_SLX

12963_SPR

42514_SPS

42567_SRM

Figure 5-3 Visual comparison between the mixtures

5.2.2 Mixture Characteristics

Table 5-3 summarizes the mixture design characteristics of each mixture, such as asphalt cement type and content, the amount of reclaimed asphalt pavement (RAP) added in each mixture, and the amount of warm-mix asphalt (WMA) additive, Evotherm. The usage of RAP in pavement construction is very attractive since it is an economical and environmentally-friendly alternative. As can be seen in the table, the percentage of RAP ranges from 30% to 50% depending on the type of mixture.

Table 5-3 Blending characteristics of mixtures selected

Mixture Type	Control Number	Binder Type	RAP (%)	Binder Content			WMA		Source
				Virgin	From RAP	Total	Content	Type	
SPH	42515	PG 64-34	35	3.38	1.82	5.2	0.70%	Evotherm	FLINTHILLS
	22586	PG 64-34	35	3.38	1.92	5.3	0.70%	Evotherm	FLINTHILLS
	42514	PG 64-34	35	3.38	1.82	5.2	0.70%	Evotherm	FLINTHILLS
SRM	42567	PG 58-34	50	2.5	2.7	5.2	0.90%	Evotherm	FLINTHILLS
SLX	M4TLOB	PG 64-34	30	3.69	1.71	5.4	0.70%	Evotherm	FLINTHILLS
	M1041	PG 64-34	30	3.95	1.55	5.5	0.70%	AD-here	FLINTHILLS
	M4TLOA	PG 64-34	30	4.02	1.38	5.4	0.70%	Evotherm	FLINTHILLS
SPR	12963	PG 64-34	35	3.38	1.82	5.2	0.70%	Evotherm	FLINTHILLS
	22454	PG 64-34	45	2.74	2.56	5.3	0.70%	AD-here	FLINTHILLS
	12980	PG 64-34	45	2.78	2.52	5.3	1.25%	HydroLime	MONARCH
	42399	PG 64-34	35	2.78	2.52	5.3	0.70%	Evotherm	MONARCH
	42567	PG 64-34	35	2.9	2.5	5.4	0.70%	Evotherm	FLINTHILLS
SPS	42399	PG 52-34	45	2.49	2.71	5.2	–	–	MONARCH
	42514	PG 52-34	45	2.86	2.34	5.2	–	–	FLINTHILLS

Note: RAP = Reclaimed Asphalt Pavement, WMA = Warm-Mixed Asphalt and – Not Applicable

5.3 Test Results and Discussion

Sample fabrication in this task followed the specimen fabrication process described earlier in chapter 3. The testing variables were selected from the recommended range shown in Table 4-1. More specifically, specimens were 50 mm thick with a notch length of 15 mm, tested at a LPD loading rate of 3 mm/min. and temperature of 21°C; in each case, results from a total of six replicates were averaged. From the test results, fracture energy was then calculated and statistical analysis conducted to assess the sensitivity of SCB test to difference in AC mixtures. The resulting values of fracture energy and the corresponding standard error bars are presented below (Figure 5-4).

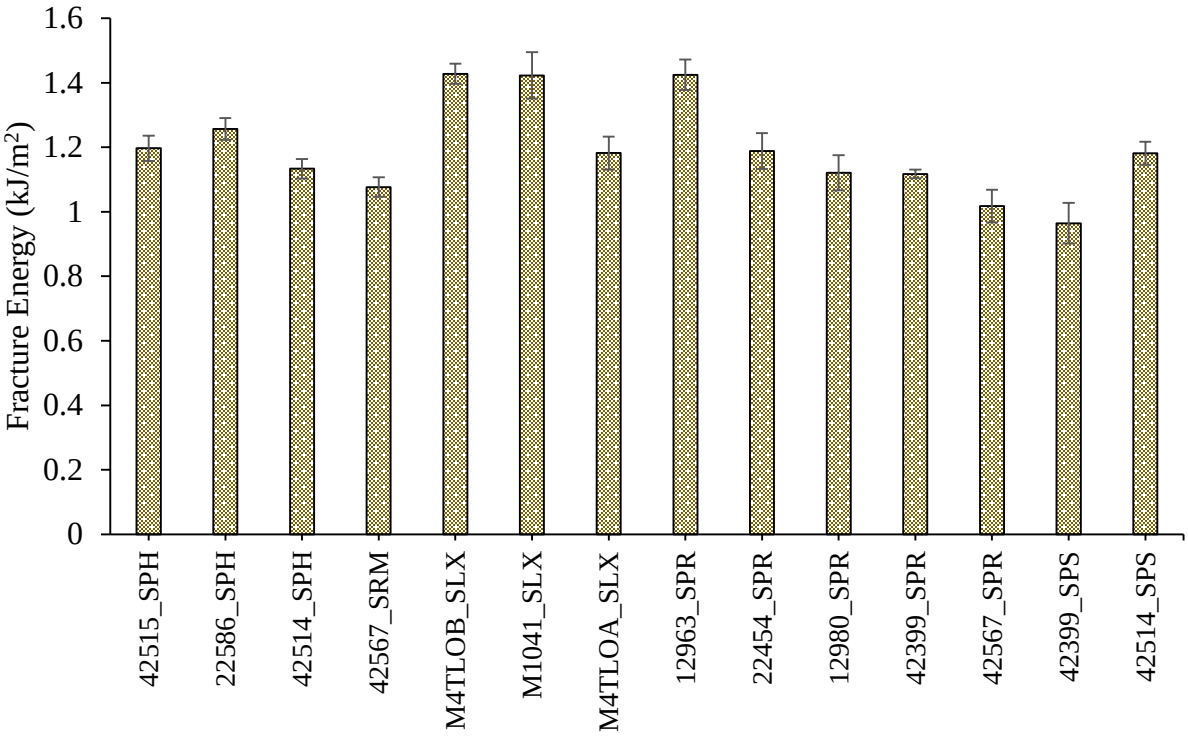

Figure 5-4 SCB test results (fracture energy) of different mixtures with standard error bars

In order to further assess the sensitivity of the SCB test method, statistical analyses were performed on the test results. For the repeatability check, the coefficient of variation (COV) from the six replicates of each mixture was estimated, and the resulting values are presented

in Table 5-4. As can be seen, the COV values of mixtures were less than 15% threshold with exception of one mixture, 42399_SPS which showed COV value of 16%. . This COV values less than 15% is explained by the fact that all testing variables in this task were chosen from the recommended values after repeatability test summarized Table 4-1. It is noteworthy that since the recommended test variables was based on statistical analysis of 95% confidence level, there is a chance (5%) that the COV may not lay in the 15% COV interval. This explains why one test with COV higher than 15%. Overall this observation further confirms the repeatability of the SCB test.

Table 5-4 Coefficient of variation of test results

Mixture Name	Coefficient of Variation (COV) of Fracture Energy
42515_SPH	8.1%
22586_SPH	6.6%
42514_SPH	6.6%
42567_SRM	6.9%
M4TLOB_SLX	5.3%
M1041_SLX	12.4%
M4TLOA_SLX	10.6%
12963_SPR	8.1%
22454_SPR	11.5%
12980_SPR	11.9%
42399_SPR	3.0%
42567_SPR	12.3%
42399_SPS	**16.0%**
42514_SPS	7.4%

Note: COV higher than 15% is marked in bold.

To further investigate the sensitivity of SCB test, an analysis of variance (ANOVA) and Tukey's honestly significant difference (HSD) multiple-comparison statistical test was conducted. In this study, the ANOVA was used to test the null hypothesis, indicating that mean values from different mixtures are equal (i.e., the alternative hypothesis indicating that at least one mean value is statistically different from other means) at a 95% confidence level. If the null hypothesis was rejected, then a post-hoc multiple-comparison analysis,

namely, Tukey's HSD was conducted. Figure 5-5 presents several available multiple-comparison tests and their corresponding powers with Type I error rates. Statistical power represents the probability of correctly detecting a difference (i.e., rejecting the null hypothesis when it is false), while Type I error is a probability of rejecting the null hypothesis when it is true (i.e., detecting false differences). The Tukey's HSD test was used herein to detect differences in mixtures due to a lower probability of a Type I error, thus less likely to detect false differences in mixtures (see Figure 5-5). The Tukey's HSD test has been used in other several studies (Zegeye, Le et al. 2012, Faruk, Hu et al. 2014) to compare AC mixtures.

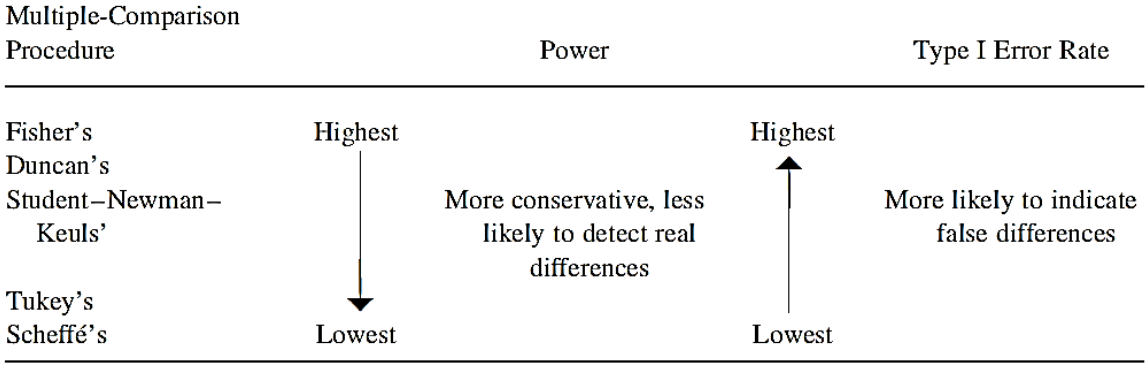

Figure 5-5 Multiple-comparison procedures (Dowdy, Wearden et al. 2011)

Since the Tukey's HSD is a post-hoc test, it requires the rejection of the null hypothesis (p-values < 0.05) to be effective and answers the question of which mean is significantly different from another.

Table 5-5 shows the ANOVA table of fracture energy resulting from the 14 mixtures. As shown, by comparing the p-value with a given α-level (0.05), the null hypothesis was

rejected, since the *p*-value is less than the α-level. This implies that at least one mixture is significantly different from other mixtures in terms of their fracture energy values at the 95% confidence level (i.e., α-level of 0.05). Consequently, the Tukey's HSD was conducted.

Table 5-5 ANOVA: single factor about fracture energy

Source of Variation	*SS*	*df*	*MS*	*F*	*P-value*	*F crit*
Between Groups	1.660773	13	0.12775184	10.053996	1.7551E-11	1.862661
Within Groups	0.88946	70	0.01270657			
Total	2.550234	83				

In Tukey's test, the number of replicates of each mixture (six in this case) and the desired probability level (i.e., 5% in this study) were first used to find the studentized *q*-value. Then the *q*-value with the variance of test results were used to find the absolute critical difference between means. If the difference between two means of mixtures is larger than the absolute critical value, the two are significantly different at that given probability level. More detailed information on Tukey's HSD test can be found elsewhere ((Dowdy, Wearden et al. 2011)).

Table 5-6 presents Tukey's HSD test results of individual mixtures with mean fracture energy values and groups (in letters). For example, two SLX mixtures (i.e., M4TLOB and M1041), a SPR mixture (12963), and a SPH mixture (22586) are ranked with the same group A due to the statistical similarity in their fracture energies with the specified confidence level (α = 0.05). As seen in the table, several mixtures are classified in group C, implying that their fracture energies are statistically similar, as previously observed in Figure 5-4.

Table 5-6 Tukey's HSD about fracture energy and mixture ranking

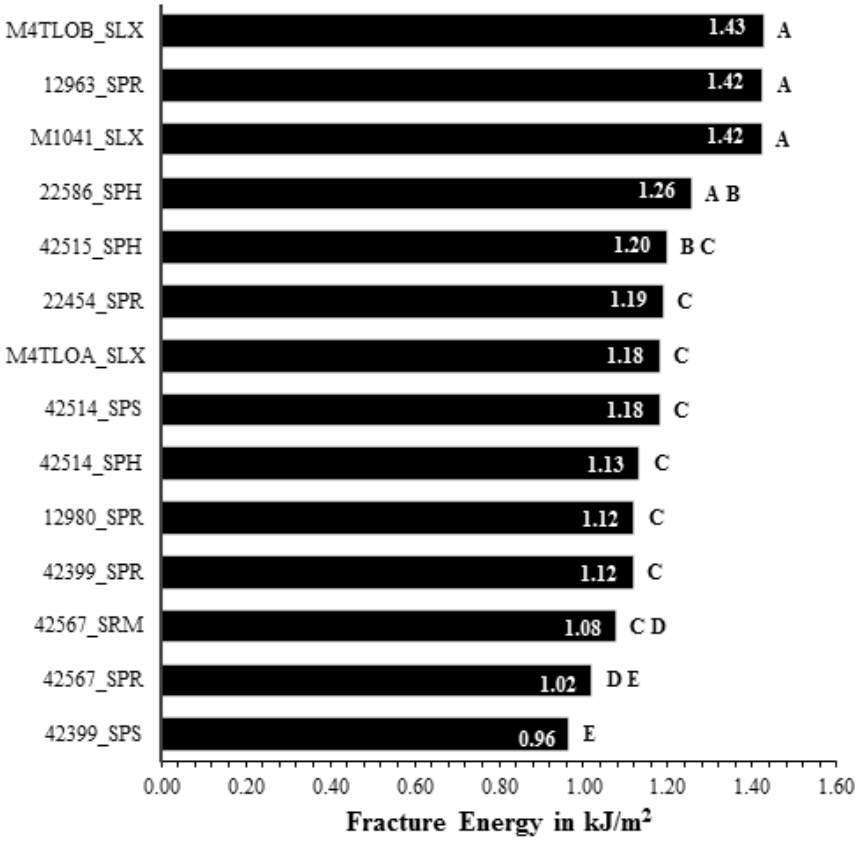

Note: Means that do not share a letter are significantly different

The above table classifies AC mixtures by ranking them in descending order (from top to bottom). In an attempt to investigate rank orders among individual AC mixture types, the Tukey's HSD test results were rewritten as shown in Table 5-7. It can be observed from the table that, among the three SLX mixtures evaluated in this study, the SLX_ M4TLOA was classified in group C with the lowest fracture energy (1.18kJ/m^2), while the other two SLX mixtures were both classified in group A with relatively high fracture energy (1.42 ~ 1.43 kJ/m^2). Among the three SPH mixtures, the SPH_22586 performed better than the other two, although it was not significantly different them implying the similarities in this mixture type. Most of SPR mixtures expect the SPR-12963 were categorized in group C or below due to their relatively low fracture energy values. As also expected, SRM and SPS were generally categorized in lower-graded groups: C to E.

Table 5-7 Mixture classification by their fracture energy

Mixture	Fracture Energy
SLX_M1041	A
SLX_M4TLOA	C
SLX_M4TLOB	A
SPH_22586	A B
SPH_42514	C
SPH_42515	B C
SPR_12963	A
SPR_12980	C
SPR_22454	C
SPR_42399	C
SPR_42567	D E
SPS_42399	E
SPS_42514	C
SRM_42567	C D

All and overall the SCB test showed acceptable sensitivity to changes in mixtures despite the highly heterogeneous nature of AC mixtures due to the added RAP materials.

5.3.1 Relationship between virgin asphalt content to fracture energy

Further results analysis was done to find the relationship between the fracture energy and mixture constituents. As result, it was observed that the fracture energy of mixtures increased with increase in virgin asphalt cement as shown in Figure 5-6 below. Virgin asphalt cement is the portion of the total asphalt content that is not from RAP materials. This portion is added to the aggregate blend containing RAP to reach a specified asphalt content by the total weight content.

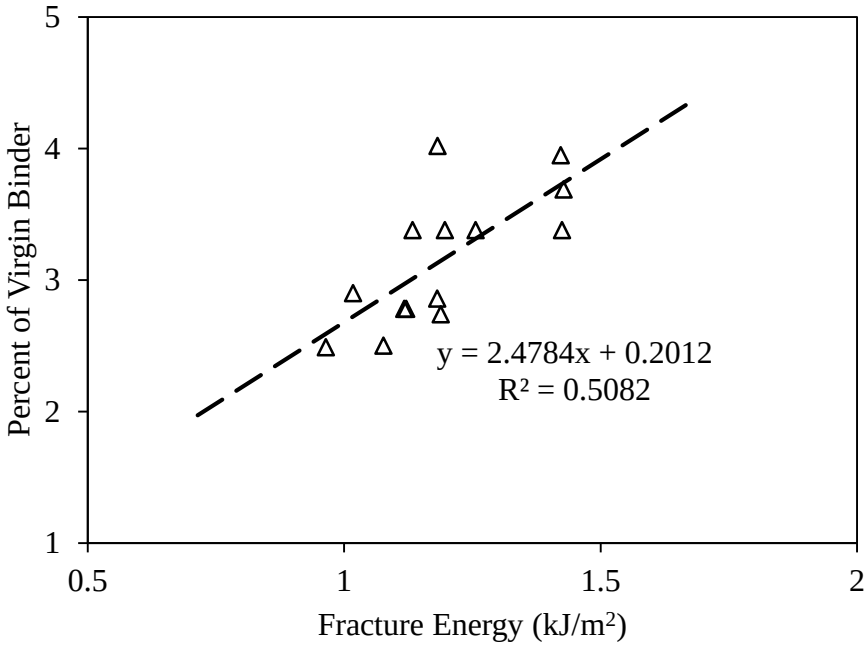

Figure 5-6 Relationship between virgin binder and fracture energy

It can inferred from this observation that fracture resistance of mixtures containing RAP materials can be increased by simply increasing the percentage of virgin asphalt content. This is reasonable since the virgin (new) asphalt provide adhesion strength that was lost in old asphalt (RAP) over the service life its service life.

CHAPTER 6 : SUMMARY AND CONCLUSIONS

With an integrated experimental-statistical approach, this thesis investigated several critical SCB testing variables (i.e., the minimum recommended number of specimens, thickness, notch length, loading rate, and testing temperature) that are considered to have a significant effect on the overall fracture behavior of AC mixtures at intermediate service temperature conditions. The first part of this research focused on development of a reliable and repeatable SCB test for AC fracture characterization. Each testing variable of the five was investigated in turn with a typical range to estimate testing repeatability and practicality. At the end of this part a range of values recommended for SCB test was presented with the associated approximate COV. The second part of this study analyzed sensitivity of the SCB testing for difference in AC mixtures. In this part, a total of 14 AC mixtures were collected from 12 different field construction projects and were tested in the University of Nebraska's Geomaterials Laboratory. Statistical analyses were then conducted to evaluate the repeatability and sensitivity of SCB test results. Based on the test-analysis results, the following conclusions can be drawn:

- The statistical analysis of a total of 18 SCB specimens indicated that five to six SCB specimens would be a reasonable sample size that can sufficiently represent asphalt concrete fracture behavior with a 95% level of confidence.
- A range of 40 mm to 60 mm for the specimen thickness showed good repeatability (COV $\leq$10%) and similar fracture energies, while the test results with 30 mm SCB thickness showed a high COV (>25%).

- Within the range of notch lengths tested in this study (0, 5, 15, 25, 40 mm), the 5 mm showed the lowest value of COV of fracture energy. However, due the resulting crack propagation profile at this notch, a 15 mm notch was recommended for SCB test.
- Fracture energy was not dependent on loading rate between 1 mm/min. to 5mm/min. and good testing repeatability (COV) was observed.
- In the range of testing temperatures attempted here, fracture energy at around 15°C showed the lowest testing variation. SCB testing at 21°C also seems attractive for practical purposes, with a little loss of testing repeatability compared to 15°C. This is because 21°C is a close to room temperature and is easily achievable with minimum temperature control equipment.
- All fracture indicators of the 14 AC mixtures from 12 separate field construction projects showed acceptable coefficient of variation (COV), generally less than 15%.
- The one-way ANOVA of fracture indicators from the 14 AC mixtures rejected the null hypothesis of equality of means of mixtures implying that at least one mixture was significantly different from others at the 95% confidence level.
- The Tukey's HSD multiple-comparison analysis result implied that overall SLX mixtures had be highest fracture energy while SPS and SRM showed the lowest values of fracture energy. This analysis showed the most of the mixtures were classified in group C.

- Overall, the SCB test developed based to the most repeatable variables was confirmed by testing the field mixtures. The developed test also showed a good sensitivity to changes in AC mixtures.
- Test results for the 14 field mixtures indicated that fracture energy increased with increasing content (percentage of the total mixture weight) of virgin asphalt.
- The findings of this study are under further evaluation for various Nebraska AC mixtures that are placed in field projects. This will lead to closer insights into the SCB fracture test through a potential quality control (QC) – quality assurance (QA) type approach to evaluate the fatigue-cracking potential of AC mixtures. Any further findings will be reported in follow-up studies.

REFERENCES

Allen, D. H., et al. (2009). "Determining Representative Volume Elements of Asphalt Concrete Mixtures Without Damage." Transportation Research Record: Journal of the Transportation Research Board **2127**(-1): 52-59.

Aragão, F. and Y.-R. Kim (2012). "Mode I fracture characterization of bituminous paving mixtures at intermediate service temperatures." Experimental Mechanics **52**(9): 1423-1434.

Aragão, F. T. S. and Y. R. Kim (2012). "Mode I Fracture Characterization of Bituminous Paving Mixtures at Intermediate Service Temperatures." Experimental Mechanics **52**(9): 1423-1434.

Biligiri, K. P., et al. (2012). "Asphalt Mixtures' Crack Propagation Assessment using Semi-Circular Bending Tests." International Journal of Pavement Research and Technology **5**(4): 209.

Brühwiler, E., et al. (1990). "Fracture of AAC as influenced by specimen dimension and moisture." Journal of Materials in Civil Engineering **2**(3): 136-146.

Chong, K. and M. Kuruppu (1984). "New specimen for fracture toughness determination for rock and other materials." International Journal of Fracture **26**(2): R59-R62.

Dowdy, S., et al. (2011). Statistics for research, John Wiley & Sons.

Duan, K., et al. (2003). "Thickness effect on fracture energy of cementitious materials." Cement and concrete research **33**(4): 499-507.

European Committee for Standardization, B., Belgium. (2010). "Bituminous mixtures—Test methods for hot mix asphalt—Part 44: Crack propagation by semi-circular bending test." (EN 12697-44: 2010).

Faruk, A. N., et al. (2014). "Using the Fracture Energy Index Concept to Characterize the HMA Cracking Resistance Potential under Monotonic Crack Testing." International Journal of Pavement Research and Technology **7**(1): 40.

Huang, B., et al. (2013). "Using notched semi circular bending fatigue test to characterize fracture resistance of asphalt mixtures." Engineering Fracture Mechanics **109**: 78-88.

Im, S., et al. (2014). "Characterization of mode-I and mode-II fracture properties of fine aggregate matrix using a semicircular specimen geometry." Construction and Building Materials **52**: 413-421.

Im, S., et al. (2014). "Mode-Dependent Fracture Behavior of Asphalt Mixtures with Semicircular Bend Test." Transportation Research Record: Journal of the Transportation Research Board(2447): 23-31.

Im, S., et al. (2013). "Rate-and Temperature-Dependent Fracture Characteristics of Asphaltic Paving Mixtures." JOURNAL OF TESTING AND EVALUATION **41**(2): 257-268.

Im, S., et al. (2013). "Rate and temperature dependent fracture characteristics of asphaltic paving mixtures." J Test Eval **41**(2): 257-268.

Kim, Y.-R. and F. T. S. Aragão (2013). "Microstructure modeling of rate-dependent fracture behavior in bituminous paving mixtures." Finite Elements in Analysis and Design **63**: 23-32.

Kim, Y.-R., et al. (2009). "Determining representative volume elements of asphalt concrete mixtures without damage." Transportation Research Record: Journal of the Transportation Research Board(2127): 52-59.

Kim, Y., et al. (2010). "Geometrical evaluation and experimental verification to determine representative volume elements of heterogeneous asphalt mixtures." JOURNAL OF TESTING AND EVALUATION **38**(6): 660-666.

Li, X. J. and M. O. Marasteanu (2009). "Using Semi Circular Bending Test to Evaluate Low Temperature Fracture Resistance for Asphalt Concrete." Experimental Mechanics **50**(7): 867-876.

Lim, I., et al. (1993). "Stress intensity factors for semi-circular specimens under three-point bending." Engineering Fracture Mechanics **44**(3): 363-382.

Liu, J. H. (2011). Fatigue life evaluation of asphalt rubber mixtures using semi-circular bending test. Advanced Materials Research, Trans Tech Publ.

Machiwal, D. and M. K. Jha (2012). Hydrologic time series analysis: Theory and practice, Springer Science & Business Media.

Marasteanu, M. O., et al. (2002). "Determining the low-temperature fracture toughness of asphalt mixtures." Transportation Research Record: Journal of the Transportation Research Board **1789**(1): 191-199.

Marasteanu, M. O., et al. (2004). "Low Temperature Cracking of Asphalt Concrete Pavement."

Paulino, G. H., et al. (2004). Cohesive zone modeling of fracture in asphalt concrete. Proceedings of the 5th International RILEM Conference–Cracking in Pavements: Mitigation, Risk Assessment, and Preservation, Limoges, France.

Razali, N. M. and Y. B. Wah (2011). "Power comparisons of shapiro-wilk, kolmogorov-smirnov, lilliefors and anderson-darling tests." Journal of Statistical Modeling and Analytics **2**(1): 21-33.

Romero, P. and E. Masad (2001). "Relationship between the representative volume element and mechanical properties of asphalt concrete." Journal of Materials in Civil Engineering **13**(1): 77-84.

Saadeh, S., et al. (2014). Correlation of Semi-circular Bending and Beam Fatigue Fracture Properties of Asphalt Concrete Using Non-Contact Camera and Crosshead Movement. T&DI Congress 2014@ sPlanes, Trains, and Automobiles, ASCE.

Shen, B. and G. Paulino (2011). "Direct extraction of cohesive fracture properties from digital image correlation: a hybrid inverse technique." Experimental Mechanics **51**(2): 143-163.

Shu, X., et al. (2010). "Evaluation of cracking resistance of recycled asphalt mixture using semi-circular bending test." Paving materials and pavement analysis (GSP 203): 58-65.

Song, S., et al. (2008). "δ25 Crack opening displacement parameter in cohesive zone models: experiments and simulations in asphalt concrete." Fatigue & Fracture of Engineering Materials & Structures **31**(10): 850-856.

Song, S. H., et al. (2005). Cohesive zone simulation of mode I and mixed-mode crack propagation in asphalt concrete. Geotechnical Special Publication No. 130: Advances in Pavement Engineering, Proceedings of Sessions of the GeoFrontiers 2005 Congress.

Wagoner, M., et al. (2005). "Investigation of the fracture resistance of hot-mix asphalt concrete using a disk-shaped compact tension test." Transportation Research Record: Journal of the Transportation Research Board(1929): 183-192.

Wagoner, M. P., et al. (2005). "Development of a single-edge notched beam test for asphalt concrete mixtures." JOURNAL OF TESTING AND EVALUATION **33**(6): 452.

Wittmann, X. and H. Zhong (1996). On some experiments to study the influence of size on strength and fracture energy of concrete, Aedificatio Verlag.

Wu, Z., et al. (2005). "Fracture resistance characterization of superpave mixtures using the semi-circular bending test." Journal of ASTM International **2**(3): 1-15.

Zegeye, E., et al. (2012). "Investigation of size effect in asphalt mixture fracture testing at low temperature." Road Materials and Pavement Design **13**(sup1): 88-101.

APPENDIX A

Location of field construction projects:

SPH :

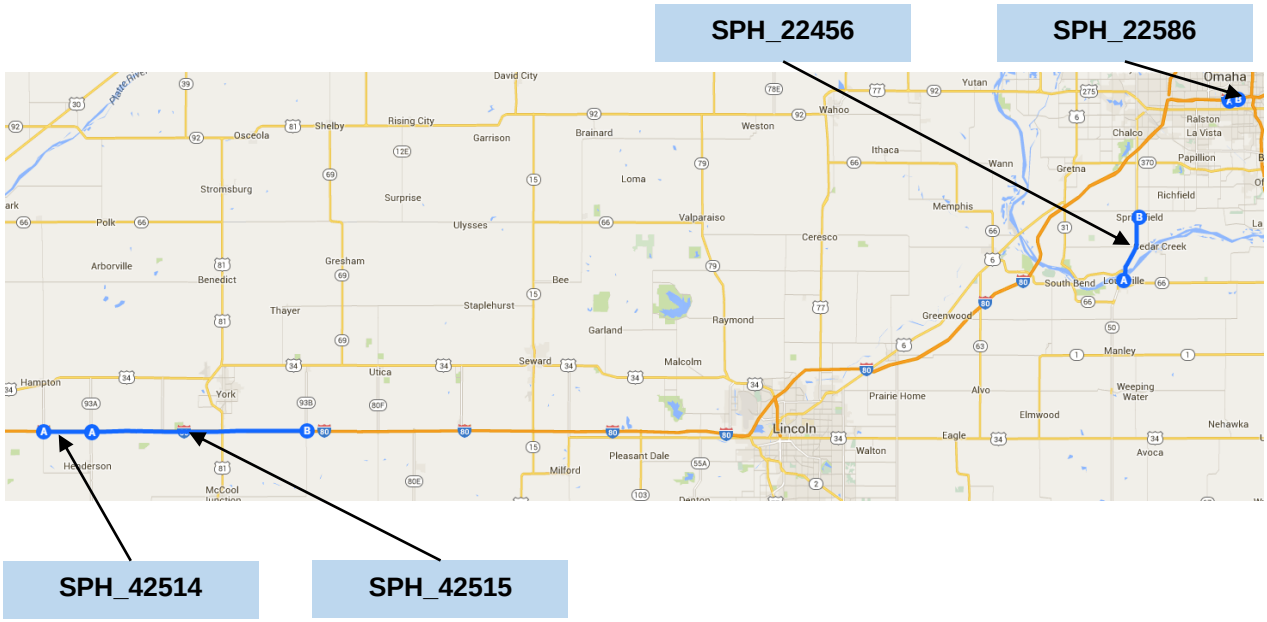

SLX :

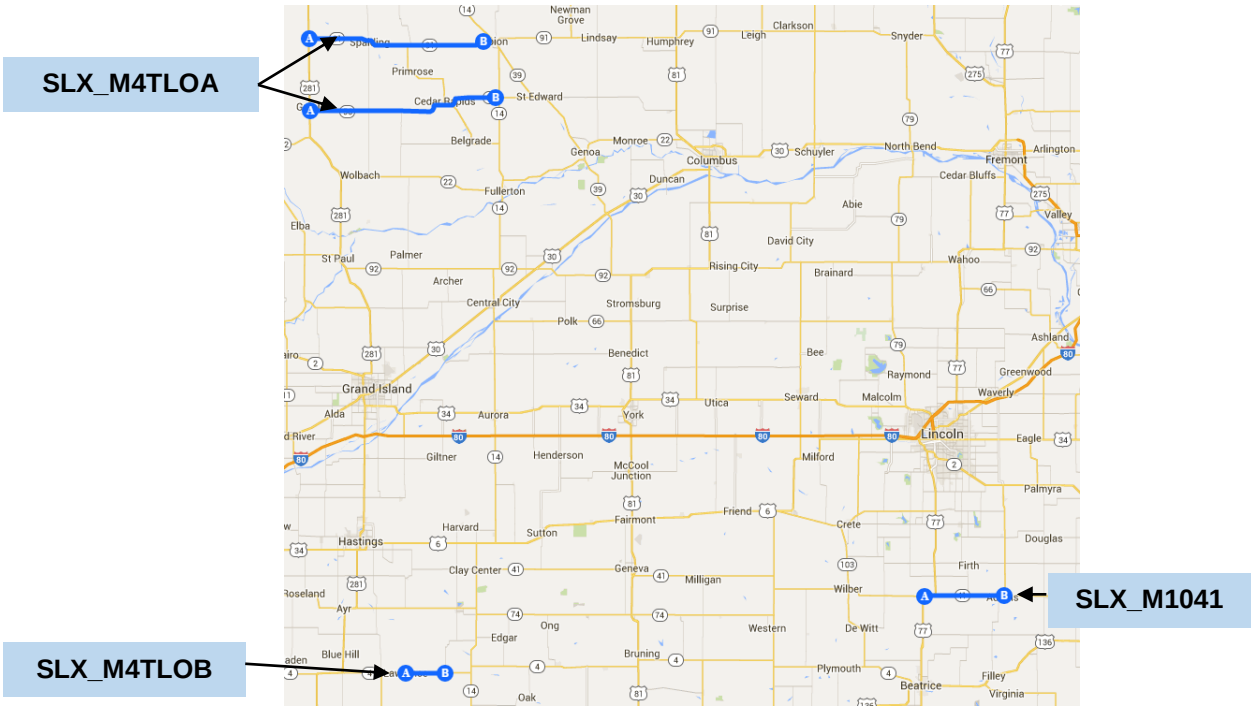

SRM :

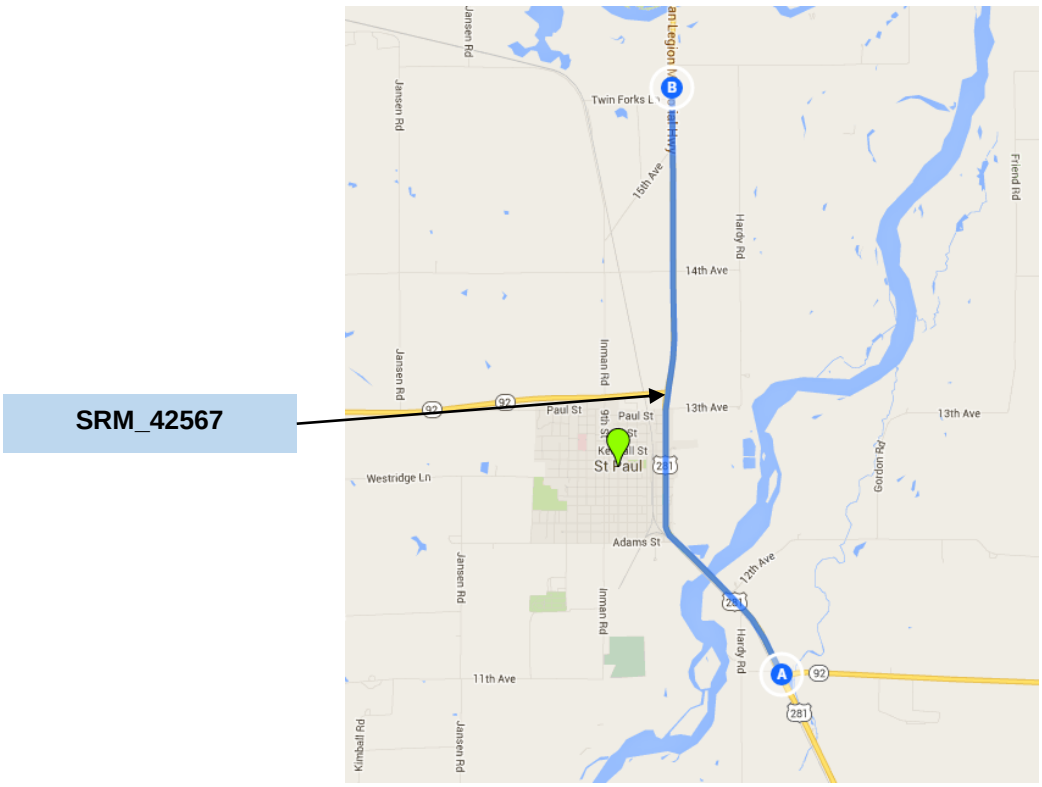
SRM_42567
Jansen Rd
Twin Forks L
15th Ave
Hardy Rd
Friend Rd
14th Ave
Inman Rd
92
Paul St
13th Ave
St Paul
281
Westridge Ln
Adams St
Gordon Rd
12th Ave
11th Ave
Kimball Rd
A
B

SPR :


SPR_42567
SPR_42454
SPR_42399
SPR_12890
SPR_13963
Grand Island
Lincoln
Omaha
Columbus
Fremont
Central City
Aurora
York
Seward
Utica
Brainard
Rising City
David City
Phillips
Hampton
Doniphan
Giltner
Henderson

SPS :

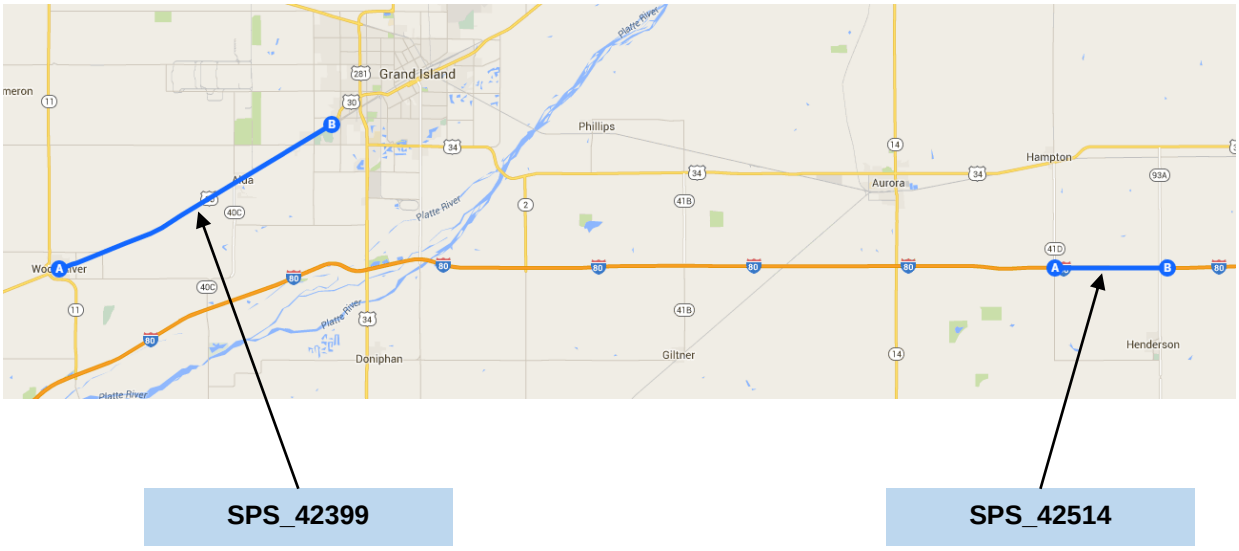
SPS_42399
SPS_42514
Grand Island
Phillips
Aurora
Hampton
Doniphan
Giltner
Henderson